Contrib Mineral Petrol (2010) 159:863–883
DOI 10.1007/s00410-009-0459-5

ORIGINAL PAPER

Migrating magmatism in the northern US Cordillera: in situ U–Pb geochronology of the Idaho batholith

Richard M. Gaschnig · Jeffrey D. Vervoort · Reed S. Lewis · William C. McClelland

Received: 2 May 2009 / Accepted: 22 October 2009 / Published online: 14 November 2009

Abstract New in situ laser ablation-inductively coupled plasma-mass spectrometry and sensitive high-resolution ion microprobe U–Pb geochronology of zircons from the Idaho batholith and spatially overlapping Challis intrusions reveals a series of discrete magmatic belts of different ages and compositions. Following the accretion of the Blue Mountains province to North America along the Salmon River suture zone, two compositionally diverse belts of metaluminous plutons formed both adjacent to the suture and well inboard of it. These were constructed from ~100 to 85 Ma and were followed by a voluminous pulse of peraluminous magmatism, forming the bulk of the Atlanta lobe and largest fraction of the batholith between ~80 and 67 Ma. Around 70 Ma, a later and more spatially restricted suite of metaluminous plutons formed around the Bitterroot lobe of the batholith. This was followed by another pulse of voluminous peraluminous magmatism in the Bitterroot lobe, lasting from ~66 to 54 Ma. The changes from low volume metaluminous to high volume peraluminous magmatism may reflect a combination of changes in the angle and segmentation of the subducting Farallon plate and over thickening of the continental lithosphere. All of these features were then cut by plutons and dikes associated with the Challis volcanic field, lasting from ~51 to 43 Ma. Inherited components are pervasive in zircons from most phases of the batholith. While Precambrian components are very common, zircons also often contain cores or mantles that are 5–20 million years older than their rims. This suggests that the early phases of the batholith were repeatedly cannibalized by subsequent magmas. This also implies that the older suites may have been originally more aerially extensive than their currently exposed forms.

Communicated by T.L. Grove.

Electronic supplementary material The online version of this article (doi:10.1007/s00410-009-0459-5) contains supplementary material, which is available to authorized users.

R. M. Gaschnig (✉) · J. D. Vervoort
School of Earth and Environmental Sciences, Washington State University, PO Box 642812, Pullman, WA 99164-2812, USA
e-mail: gaschnig@wsu.edu

R. S. Lewis
Idaho Geological Survey, University of Idaho, PO Box 443014, Moscow, ID 83844-3014, USA

W. C. McClelland
Department of Geoscience, University of Iowa, 121 Trowbridge Hall, Iowa City, IA 52242, USA

Introduction

The Idaho batholith (Fig. 1) is a major silicic magmatic center in the North American Cordillera and occurs at several unique and important tectonic junctions. The batholith was emplaced entirely in Precambrian continental crust adjacent to the Salmon River suture zone (e.g., Lund and Snee 1988), a major lithospheric boundary between accreted terranes of island-arc affinity to the west and Precambrian continental North American crust to the east that is characterized by an extremely sharp isotopic gradient interpreted to reflect the vertical geometry of this lithospheric-scale structure (e.g., Manduca et al. 1992). The batholith also occurs at an important transition zone along the strike of the Cordillera between the Laramide tectonic regime to the south and east and thin-skinned Canadian tectonic regime to the north (e.g., Armstrong 1988; Burchfiel et al. 1992; Saleeby 2003; Gehrels et al. 2009). The former was characterized by an abrupt shutoff of continental margin magmatism and development of

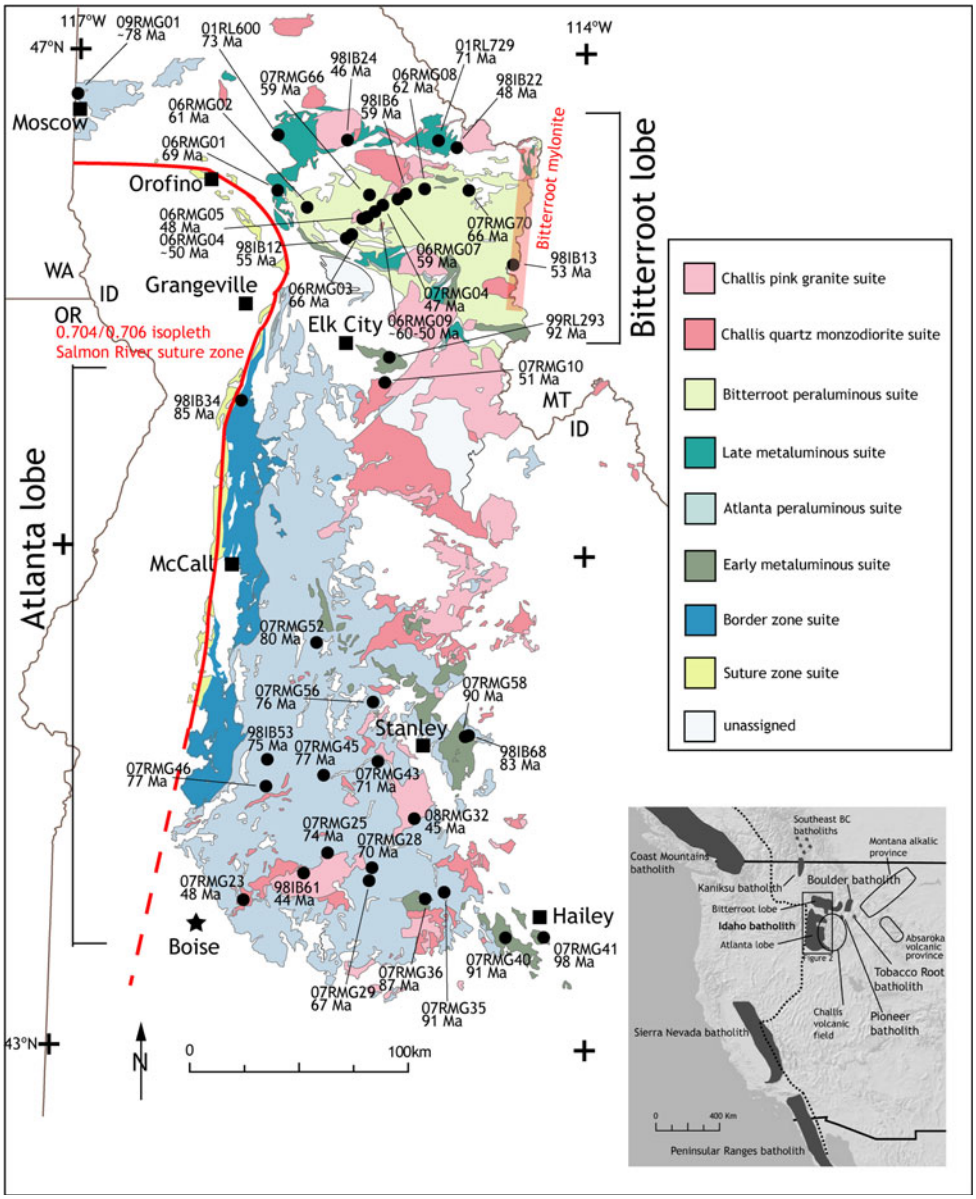

Fig. 1 Generalized geologic map of Idaho batholith, showing major lithological suites, sample locations, and ages (rounded to the nearest Ma). *Inset* shows Idaho batholith in the context of other Cordilleran batholiths. See online version for color map

basement-cored uplifts and scattered magmatic centers in the foreland. The latter is characterized by more or less continuous magmatism during latest Cretaceous and early Tertiary time. The Idaho batholith, when taken together with the spatially overlapping Challis magmatic province, represents a 70-million year record of magmatism during periods of both regional compression and extension. For these reasons, the batholith represents a key to understanding the interaction between tectonics and magmatism in the Cordillera. In spite of this important tectonic location, the Idaho batholith has been the subject of far less work than the intensively studied Sierra Nevada and Peninsular Range batholiths and to a lesser extent the Coast Mountains batholith. Most significantly, the ages of the major components of the Idaho batholith are not well constrained. This results from, in large part, the complex U–Pb systematics in its zircons due to pervasive inheritance (Chase et al. 1978; Bickford et al. 1981; Shuster and Bickford 1985; Toth and Stacey 1992).

In this contribution, we have used in situ laser ablation-inductively coupled plasma-mass spectrometry (LA-ICP-MS) and sensitive high-resolution ion microprobe (SHRIMP) U–Pb analysis of zircon for age determinations of 40 previously undated samples from various parts of the Idaho batholith. These methods, when guided by scanning electron microscope in cathodoluminescence (SEM-CL) imaging, enable us to date individual age domains in zircons and avoid inherited cores that have been problematic in previous studies. In total, the new ages presented here establish the most complete U–Pb chronology of the

assembly of the batholith and subsequent Eocene Challis magmatic flare-up to date.

Geological setting

The Idaho batholith (Fig. 1) is located east of the Salmon River suture zone and intrudes Mesoproterozoic Belt Supergroup and Neoproterozoic (Windermere equivalent) metasedimentary rocks (Hyndman 1983; Lund et al. 2003). The age and nature of the basement on which these sediments were deposited is poorly constrained but appears to be a Paleoproterozoic composite terrane, termed the Wallace terrane by Sims et al. (2005) and Selway terrane by Foster et al. (2006). Archean crust, identified in mid-crustal xenoliths (Leeman et al. 1985; Wolf et al. 2005), is present to the south beneath the Snake River Plain and probably extends under the southernmost Idaho batholith (Link et al. 2007; Gaschnig et al. 2008). Late Archean and Paleoproterozoic orthogneisses have also been recently identified along the northern fringe of the Idaho batholith (Brewer et al. 2008).

The western boundary of the batholith is defined by the Salmon River suture zone and this structure is intruded by small, discrete bodies ranging from quartz diorite to tonalite and granodiorite. These plutons are variably deformed and units include the Little Goose Creek complex north of McCall (Manduca et al. 1992) and tonalite and quartz diorite plutons east and southeast of Orofino (Kauffman et al. 2006; Lewis et al. 2007a). Most of these plutons have isotopic characteristics similar to the accreted Blue Mountains province or transitional between it and continental North America (Manduca et al. 1992; Fleck and Criss 2004). It is unclear whether these plutons are completely autochthonous in relation to the Idaho batholith and consequently whether they should be considered part of the batholith. For the sake of completeness, we show these in Fig. 2 as the *suture zone suite* but do not discuss them in depth in this paper for the reasons given above and because we do not present any new data for them.

Immediately east of, and parallel to, the suture zone and intruding continental crust is a series of narrow, tabular tonalite, granodiorite, and quartz diorite plutons. An example of this type of pluton is the Payette River tonalite, described in detail by Manduca et al. (1992, 1993). These rocks generally display a steeply dipping fabric and have geometries and an apparent tectonic setting comparable to the sheeted tonalite plutons in the Coast Mountains batholith of British Columbia and southeastern Alaska (McClelland et al. 2000). Like the suture zone suite, hornblende and also magmatic epidote are usually present in these rocks. We refer to these units collectively as the *border zone suite* (Fig. 2), consistent with the similar designation given by Taubeneck (1971).

The main body of the Idaho batholith has traditionally been divided up into the larger Atlanta lobe to the south and smaller Bitterroot lobe to the north, separated by a zone of metamorphic rocks originally named the Salmon River arch and inferred to represent a pre-Belt basement high (Armstrong 1975b) but more recently recognized to consist of metamorphosed Belt rocks and slightly younger Mesoproterozoic intrusions (Evans and Zartman 1990; Doughty and Chamberlain 1996). The two lobes generally lack the continuous mappable internal contacts found in other Cordilleran batholiths that are interpreted to represent discrete bodies of magma. For this reason, we divide the rocks of the two lobes into a few large suites based on age, petrography, and major element chemistry (Fig. 1; Table 1). The divisions, as defined below, are the early and late metaluminous suites and the Atlanta and Bitterroot peraluminous suites.

The eastern margin of the Atlanta lobe contains a fringing belt of discrete metaluminous, hornblende-bearing plutons, often containing mafic enclaves. In the southeastern Atlanta lobe these consist of a group of granodiorite-to-quartz diorite stocks noted for their relatively high K_2O for a given SiO_2 content (Kiilsgaard et al. 2001). In the east-central Atlanta lobe a belt of distinctive porphyritic plutons, with poikilitic K-feldspar megacrysts up to 10 cm long, extends from Stanley northwest toward McCall, before trending northeast to Elk City. From Stanley to McCall, the megacrystic bodies occupy areas of higher elevation and may be roof pendants or remnants of a more extensive series of plutons. Slivers of augen gneiss in the western (augen gneiss of Apgar Creek of Lund et al. 2008) and north-central parts of the Bitterroot lobe may represent deformed continuations of this unit (K. Lund, personal communication). We refer to these rocks collectively as the *early metaluminous suite*.

Another belt of metaluminous rocks forms a perimeter surrounding the Bitterroot lobe. This belt includes the Skookum Butte quartz diorite and Toboggan Ridge stock along the northern edge of the Bitterroot lobe and a large quartz diorite mass on the western and northwestern edge. We refer to these collectively as the *late metaluminous suite*.

The Idaho batholith is dominated by vast volumes of peraluminous granitoids. In the Atlanta lobe, this consists of a ubiquitous and relatively homogeneous biotite granodiorite, which is cored by a muscovite–biotite granite/granodiorite and cut by dikes and small masses of biotite leucogranite. All of these units are weakly to strongly peraluminous and show only limited internal geochemical and petrographic variation (Lewis et al. 1987). Hornblende and mafic microgranular enclaves are absent, although mica-rich enclaves of possible metasedimentary origin are locally present. Muscovite is thought to be magmatic based

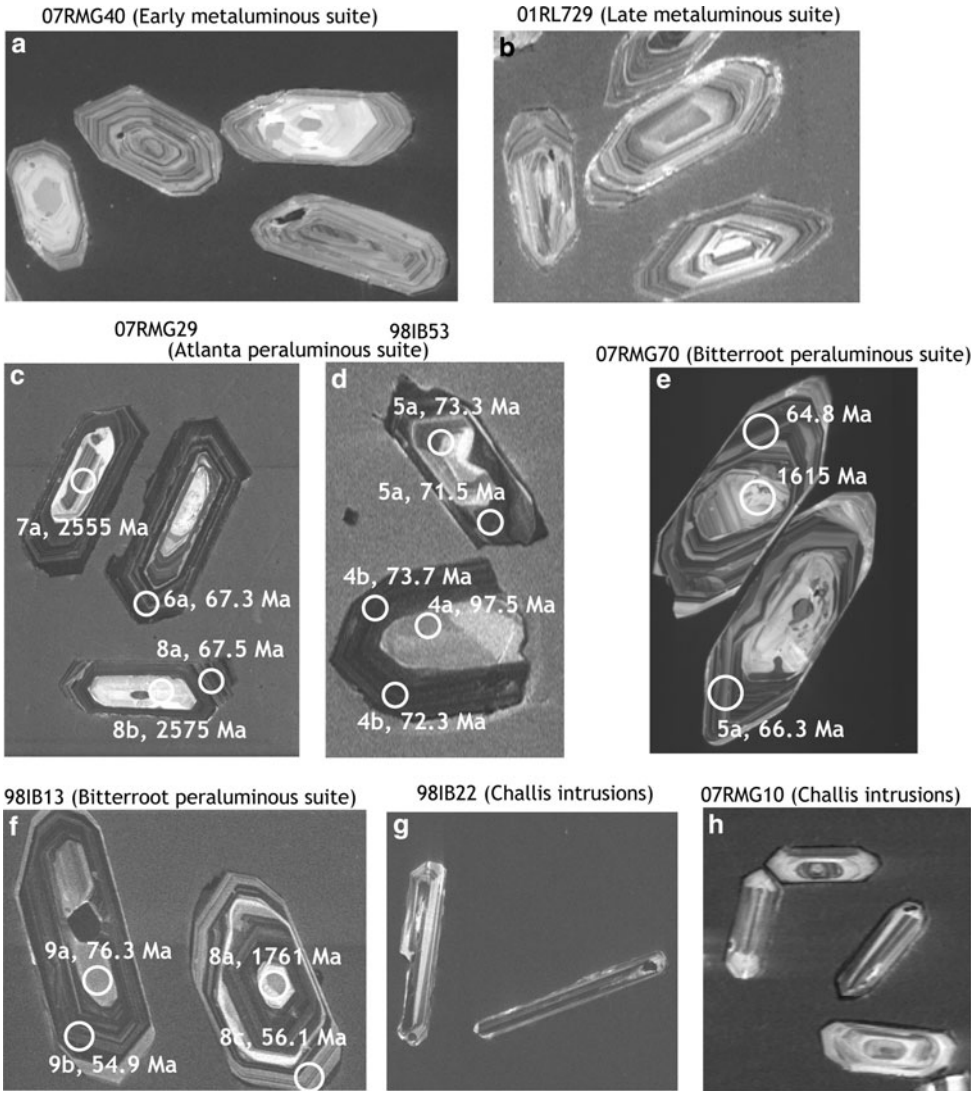

Fig. 2 SEM-CL images of zircons from the different lithological suites, showing examples of zoning and inheritance patterns. Individual analytical spots and ages are labeled for the zircons from the peraluminous suites in order to illustrate the great complexity these zircons exhibit

on textural criteria (Kiilsgaard and Lewis 1985), although no compositional data have been published. Together, we refer to these units in the Atlanta lobe, and temporally and compositionally correlative outliers elsewhere in Idaho, as the *Atlanta peraluminous suite*.

The peraluminous interior of the Bitterroot lobe is dominated by biotite granodiorite that is broadly similar, petrographically and geochemically, to the corresponding unit of the Atlanta lobe (Lewis and Stanford 2002). The muscovite-bearing granite, however, is less abundant and is commonly found in close proximity to metasedimentary wallrock screens. Outcrop scale textural heterogeneities are more common when compared to the Atlanta peraluminous suite (Hyndman 1984). Mafic dikes, sills, and small intrusions that have been interpreted to be co-magmatic with the granitoids are also present in this unit (Hyndman and Foster 1988; Foster and Hyndman 1990) while absent in the Atlanta peraluminous suite. Herein, we refer to the peraluminous main phases of the Bitterroot lobe as the *Bitterroot peraluminous suite* (Fig. 1).

All of the phases of the Idaho batholith discussed above are intruded by epizonal plutons and dikes associated with the Challis volcanic field (Armstrong 1974) of east-central and southeastern Idaho (Fig. 1). These intrusions form discrete stocks of various sizes commonly containing miarolitic cavities and intruding coeval volcanic piles in a few areas (e.g., Larson and Geist 1995). They are divided into two suites. *The quartz monzodiorite* suite has a wide range of lithologies from gabbro to granite, generally contains hornblende, and has a color index >10. The *pink granite* suite is restricted to granite sensu stricto and occasional syenite, typically contains little or no hornblende, and has distinctive major and trace element signatures characteristic of A-type granites (Lewis and Kiilsgaard 1991).

Table 1 Sample locations and general characteristics

Sample	Lithology	Location	Latitude	Longitude (NAD27)	SiO_2[a]	ASI[a]
Border zone suite (2,100 km^2)						
98IB34	Tonalite	Slate Creek	45.6269	−116.0208	67.46	1.02
Early metaluminous suite (1,300 km^2)						
07RMG41	px-bt diorite	Croesus Gulch	43.4713	−114.3465	55.73	0.79
99RL293	Megacrystic hbl-bt granodiorite	Elk City	45.7804	−115.1932	–	–
07RMG40	bt-hbl granodiorite	Richardson Summit	43.4495	−114.4400	62.76	0.90
07RMG35	bt granodiorite	Big Smokey Cr	43.6037	−114.8595	69.87	1.02
07RMG58	Megacrystic hbl-bt granite	Stanley area	44.2668	−114.7572	64.79	0.88
07RMG36	hb-bt tonalite	South Fork of Boise R	43.5912	−114.9583	66.15	0.97
Atlanta peraluminous suite (16,000 km^2)						
98IB68	bt tonalite	Stanley area	44.2678	−114.7561	73.36	1.09
07RMG52	bt-ms granite	Warm Lake	44.6416	−115.6272	74.47	1.09
07RMG45	bt granodiorite	Lowman area	44.0708	−115.5381	72.24	1.08
07RMG46	bt granodiorite	Lowman area	44.0504	−115.8909	72.67	1.06
07RMG56	bt granodiorite	Cape Horn Summit	44.3576	−115.2356	73.38	1.03
07RMG25	bt granodiorite	Middle Fork of Boise R	43.7805	−115.4927	72.76	1.03
98IB53	ms-bt granodiorite	Middle Fork of Payette R	44.2189	−115.9161	76.36	1.28
07RMG43	bt leucogranite	Grandjean	44.1722	−115.2441	72.62	1.04
07RMG28	bt granodiorite	N of Rocky Bar	43.7525	−115.2442	73.56	1.07
07RMG29	bt granodiorite	Rocky Bar	43.6840	−115.2787	74.54	1.08
09RMG01	bt-ms granite	Moscow Mountain	46.8097	−117.0070	–	–
Late metaluminous suite (1,100 km^2)						
01RL600	qtz diorite	Headquarters	46.6639	−115.8593	61.90	0.91
01RL729	bt-hbl granodiorite	Toboggan Ridge	46.6680	−115.0254	63.59	0.98
06RMG01	qtz diorite	Wieppe	46.3929	−115.8553	63.81	0.98
Bitterroot peraluminous suite (2,100 km^2)						
07RMG70	ms-bt granite	Tom Beal Park	46.4459	−114.7312	72.74	1.11
06RMG03	bt-ms granodiorite	Lochsa R (Black Canyon)	46.2865	−115.3839	72.56	1.09
06RMG08	Porphyritic bt granodiorite	Lochsa R (Weir Cr)	46.4593	−115.0383	72.41	1.06
06RMG07	Porphyritic bt granodiorite	Lochsa R (Castle Cr)	46.4150	−115.1740	71.94	1.05
07RMG66	Porphyritic bt granite	Lolo Trail	46.4269	−115.2899	71.21	1.08
98IB6	ms-bt qtz monzodiorite	Lochsa R (Skookum Cr)	46.4219	−115.1475	72.33	1.03
98IB12	Monzogranite in migmatite zone	Lochsa R (Black Canyon)	46.2842	−115.3881	76.43	1.05
98IB13	Foliated ms-bt qtz monzonite	Bitterroot Mtns	46.1469	−114.5011	73.57	1.02
06RMG02	bt granodiorite	Lolo Cr	46.3793	−115.7130	72.11	1.12
06RMG09	bt granodiorite	Lochsa R (Noseeum Cr)	46.3587	−115.2846	74.00	1.04
Challis intrusions (8,500 km^2)						
07RMG10	hb-px granodiorite	western Nez Perce Trail	45.6949	−115.2330	69.04	0.99
06RMG05	hbl-bt syenite	Lochsa R (Fish Cr)	46.3315	−115.3457	66.06	0.99
98IB22	Dacite porphyry dike	Lolo Trail	46.6044	−114.8811	68.53	0.97
07RMG23	bt-hbl monzodiorite	Lucky Peak Reservoir	43.5929	−115.9545	65.72	0.95
07RMG04	qtz diorite hybrid	Lochsa R (Bald Mtn Cr)	46.3868	−115.2318	60.55	0.89
98IB24	Pink bt granite	N Fork of Clearwater R	46.6861	−115.3625	71.36	1.08
08RMG32	Pink bt granite	Sawtooth Range	43.9651	−114.9674	77.23	1.04
98IB61	Pink bt granite	Boise R (Twin Springs)	43.7128	−115.6278	75.71	1.04
06RMG04	bt granodiorite	Lochsa R (Fish Creek)	46.3315	−115.3457	74.57	1.09

ASI is molar Al/(K + Na + Ca)

qtz Quartz, *ms* muscovite, *bt* biotite, *hbl* hornblende, *px* pyroxene

[a] SiO_2 and ASI values determined by XRF at Washington State University Geoanalytical Laboratory with the exception of samples beginning with "98-". Values for those samples are from King and Valley (2001)

Previous geochronology

Some of the earliest attempts to establish the geochronological relations of the Idaho batholith were made by Armstrong (1974, 1975a) and Armstrong et al. (1977) using K–Ar and Rb–Sr methods. These, and additional K–Ar and Ar–Ar results by Criss et al. (1982), Criss and Fleck (1987), Lewis et al. (1987), Snee et al. (1995), Fleck and Criss (2004), and Snee et al. (2007), established a general Cretaceous age for the Idaho batholith proper and Eocene age of later epizonal intrusions and provided great insight into regional patterns of exhumation and uplift. Because of the systems used, however, many of these represented cooling ages and not necessary the crystallization ages of the plutons. Areas around the Eocene epizonal plutons were found to be especially prone to thermal resetting due not only to direct conductive heating but also to the induced circulation of hydrothermal fluids (Criss et al. 1982).

Attempts to directly date parts of the batholith using the U–Pb chronometer in zircon by ID-TIMS (isotopic dilution-thermal ionization mass spectrometry) have been relatively few in number, generally with complicated results. In studies of the northeastern fringe of the Bitterroot lobe, Chase et al. (1978), Bickford et al. (1981), and Shuster and Bickford (1985) encountered a pervasive Precambrian inherited zircon component and could only provide loose age constraints of crystallization times ranging from 82 to 60 Ma. This part of the batholith was re-examined by House et al. (2002), who also encountered complexities in the Skookum Butte pluton and epizonal Lolo Hot Springs batholith and Whistling Pig stock. Toth and Stacey (1992) sampled over a larger area in the Bitterroot lobe, and although they encountered similar zircon complexities, they found evidence that much of the interior of the Bitterroot lobe was younger (Paleocene) than previously thought. Attempts to date marginal portions of the Atlanta lobe by ID-TIMS were more successful. L. Fischer (written communication in Lewis et al. 1987) reported a near-concordant zircon date of 88 ± 6 Ma from the porphyritic granodiorite east of Stanley, and Manduca et al. (1993) obtained a concordant date of 90 ± 5 for the Payette River tonalite of the border zone suite and discordant dates of 110 ± 5 and 118 ± 5 Ma for the Little Goose Creek orthogneiss and Hazard Creek complex of the suture zone suite near McCall. More recent work on plutons in and adjacent to the suture zone around McCall, and in the vicinity of Orofino and Grangeville, by both ID-TIMS and in situ methods, have yielded a range of ages from 125 to 90 Ma (McClelland and Oldow 2007; Giorgis et al. 2008; Unruh et al. 2008).

Foster and Fanning (1997) and Foster et al. (2001, 2007a) were the first to use in situ U–Pb geochronology by SHRIMP to circumvent the problematic inheritance in Idaho batholith zircons in an attempt to understand the relationship between magmatism and the development of the Bitterroot metamorphic core complex. Their sampling was primarily focused on the structurally complex rocks of the Bitterroot Range, and they found that zircons from these units contained inherited cores of both Precambrian and latest Cretaceous age. Their interpreted crystallization ages based on zircon rims were mostly between 64 and 54 Ma. This seemed to confirm the suggestion of Toth and Stacey (1992) that the main phase of magmatism in the Bitterroot lobe occurred during the Paleocene.

To summarize, the ages of intrusive rocks in and adjacent to the Salmon River suture zone are relatively well constrained due to the relatively simple nature of their zircons. In contrast, the ubiquitous zircon inheritance in the main phases of the batholith makes an in situ approach essential. Aside from this contribution, no in situ geochronology exists for the Atlanta lobe and only a limited number of in situ dates have been published for the Bitterroot lobe.

Methods

Rock samples were collected in quantities of 5–10 kg. Zircons were isolated using standard crushing and mineral separation procedures. Grains handpicked under a binocular microscope were mounted in epoxy with standards, polished to expose their centers, carbon-coated, and imaged with a SEM in CL mode at the University of Idaho. Representative CL images are shown in Fig. 2. Samples with the prefix "98IB" were obtained from E. King and J. Valley, who analyzed separates of zircon and other minerals for oxygen isotopes (King and Valley 2001; King et al. 2007).

LA-ICP-MS

All LA-ICP-MS U–Pb analyses were conducted at Washington State University using a New Wave Nd:YAG UV 213-nm laser coupled to a ThermoFinnigan Element 2 single collector, double-focusing, magnetic sector ICP-MS. Operating procedures and parameters are discussed in greater depth by Chang et al. (2006) and are only briefly outlined here. Laser spot size and repetition rate were 30 μm and 10 Hz, respectively. He and Ar carrier gases delivered the sample aerosol to the plasma. Each analysis consisted of a short blank analysis followed by 300 sweeps through masses 204, 206, 207, 208, 232, 235, and 238, taking approximately 35 s.

Laser ablation-inductively coupled plasma-mass spectrometry isotopic analyses are affected by two forms of inter-element fractionation that must be corrected (e.g., Kosler and Sylvester 2003). Time-dependent fractionation occurs due to the more efficient volatilization of Pb over U as the laser excavates successively deeper levels in the ablation pit during an analysis which, in turn, leads to an increase in $^{206}Pb/^{238}U$ and $^{207}Pb/^{235}U$ ratios with time (Eggins et al. 1998). It has been demonstrated that U/Pb fractionation is approximately linear over the short time of the analysis (Kosler and Sylvester 2003). By definition, time-dependent fractionation is zero at the beginning of the analysis. Regression of time series data to the intercept at $t = 0$, therefore, yields the point at which time-dependent fractionation equals zero.

Time-independent (or static) fractionation is the largest source of uncertainty in LA-ICP-MS U–Pb geochronology and results from mass and elemental static fractionation in the plasma and also poorly understood laser-matrix effects (Kosler and Sylvester 2003). It is corrected by normalizing U/Pb and Pb/Pb ratios of the unknowns to the zircon standards (Chang et al. 2006). For this study we used two zircon standards: Peixe, with an age of 564 Ma (Dickinson and Gehrels 2003), and FC-1, with an age of 1,099 Ma (Paces and Miller 1993). Peixe was used to correct the $^{238}U/^{206}Pb$ and $^{235}U/^{207}Pb$ ratios and FC-1 was used to correct the $^{207}Pb/^{206}Pb$ ratios.

Common Pb can represent a proportionally large contribution to the total Pb in Mesozoic and younger U-poor zircons. However, common Pb is typically not significant in LA-ICP-MS analyses, most likely because it is concentrated in cracks and inclusions, which can be avoided. When this is not possible, the influence of common Pb is easy to recognize on Tera–Wasserburg diagrams because analyses tend to line up on a steep linear trajectory that can be anchored at a reasonable $^{207}Pb/^{206}Pb$ common lead composition (y-intercept = 0.86, DeGraaff-Surpless et al. 2002). Common Pb corrections were made on these analyses using the ^{207}Pb method (Williams 1998).

Uranium–lead data were reduced using Isoplot (Ludwig 2003). The final crystallization ages that we report are weighted mean $^{206}Pb/^{238}U$ ages, which were determined using the following procedure. In most of our samples, the majority of analyses form a single dominant cluster around a single spot on or just above concordia in Tera–Wasserburg space, which we interpret to be the approximate age of the sample. Analyses that gave $^{207}Pb/^{206}Pb$ ages overlapping in uncertainty with their $^{206}Pb/^{238}U$ ages were judged to be concordant. In the small number of cases where a few concordant analyses yielded younger ages that were clear outliers, we rejected these because Cretaceous and younger zircons that have experienced minor lead loss will commonly still yield concordant but slightly younger ages. We then used the $^{206}Pb/^{238}U$ ages of the concordant analyses and those corrected for common lead to calculate a weighted $^{206}Pb/^{238}U$ crystallization age.

Uncertainties on individual analyses quoted at the 2σ level are based on in-run uncertainty only (estimated by the standard error of the sample analysis) and these uncertainties were used to calculate the weighted mean. The reproducibility of the bracketing standards (as represented by the standard deviation of the analyses of standards that bracket the unknowns) was then added quadratically to the weighted mean two sigma error. An alternate method of uncertainty treatment is to add the uncertainty from the standards to each individual unknown and then calculate the weighted mean, but the pooling of analyses for the weighted mean calculation tends to reduce the uncertainty to unrealistically low levels, often lower than the reproducibility of the standards, which cannot truly be the case. The one drawback of the method we use is that the MSWD values from the weighted mean calculations tend to be unrealistically high (up to 10) because the uncertainty from the standards is excluded for the individual analyses. The ages that we report in Table 2 are each followed by two uncertainties: the first is derived from the weighted mean calculation alone and the second represents our preferred uncertainty, with the error from the standards quadratically added to the weighted mean error. The ages discussed in text are expressed only with the larger total uncertainty. We also include the internal MSWD values in Table 2 for completeness but emphasize for reasons mentioned above that they are largely *qualitative* measures of scatter.

Data plots for all samples are shown in Appendix A in Electronic Supplementary Material and tabulated results for individual spots are shown in Appendix C in ESM. Due to the large number of ages presented in this paper, we only depict some representative data plots in Fig. 3.

The ages of Precambrian inherited zircon cores in our samples will only be briefly summarized here and will be discussed and interpreted in another contribution.

SHRIMP

Sensitive high-resolution ion microprobe-reverse geometry (SHRIMP-RG) analyses were conducted at the United States Geological Survey, Stanford University Ion Probe Laboratory, Stanford, CA. Concentration calibrations were based on analyses of zircon standard CZ3 (238 ppm U). Isotopic compositions were calibrated by replicate analyses of zircon standard R33 (419 Ma; Black et al. 2004) with a calibration error for the $^{206}Pb/^{238}U$ ratios of R33 of 0.63% (2σ). The analytical routine followed Williams (1998) and Barth et al. (2001). Data reduction and plotting utilized programs of Ludwig (2001, 2003). U–Pb data for the sample dated by SHRIMP-RG is plotted on a Tera–Wasserburg diagram and weighted $^{206}Pb/^{238}U$ age diagram in Appendix A in ESM and

Table 2 Summary of ages presented in this paper

Sample	$^{206}Pb/^{238}U$ Age	In-run error[a]	MSWD[b]	Final error[c]	pC cores[d]	Comments
Border zone suite						
98IB34	85.0	±1.5	4	±2.1	Yes	7 Ma spread
Early metaluminous suite						
07RMG41	98.2	±0.9	5.2	±2.1	No	7 Ma spread
99RL293	92.4	±0.6	0.6	±0.8	Yes	Older Cretaceous zones
07RMG40	91.4	±1.0	10.5	±2.6	No	9 Ma spread
07RMG35	90.9	±1.5	2.6	±1.8	Yes	Younger outlier
07RMG58	89.8	±0.7	1.3	±1.1	No	Simple
07RMG36	86.7	±1.0	2.3	±2.8	Yes	Younger outliers
Atlanta peraluminous suite						
98IB68	82.9	±1.2	3.8	±1.9	yes	Older Cretaceous cores
07RMG52	80.2	±0.7	1	±1.5	No	Some low U zones
07RMG45	76.8	±1.6	6.7	±2.1	Yes	Older Cretaceous cores
07RMG46	76.9	±1.7	9.6	±2.9	Yes	Older Cretaceous core and grain
07RMG56	76.3	±1.6	4.5	±2.6	No	Older Cretaceous cores
07RMG25	74.0	±0.9	6.9	±2.4	Yes	Older Cretaceous cores and mantles
98IB53	74.6	±1.1	4.5	±1.7	Yes	Older Cretaceous cores
07RMG43	71.2	±1.1	1.4	±2.0	Yes	Cretaceous mantles
07RMG28	69.8	±1.1	6.8	±1.7	Yes	Older Cretaceous cores; 1 young outlier
07RMG29	67.2	±0.7	6.4	±1.6	Yes	Older Cretaceous cores; 2 young outliers
09RMG01	~78				Yes	Older Cretaceous cores; large scatter in rim ages
Late metaluminous suite						
01RL600	73.1	±0.7	1.6	±3.7	Yes	Simple
01RL729	71.3	±0.9	3.2	±1.6	Yes	Simple
06RMG01	68.9	±1.2	3.5	±2.8	Yes	6 Ma spread
Bitterroot peraluminous suite						
07RMG70	65.9	±1.0	4	±3.5	Yes	3 Younger outliers
06RMG03	65.6	±0.5	1.3	±3.6	Yes	Cretaceous cores and mantles; 2 younger rim outliers
06RMG08	61.9	±0.8	4.5	±2.8	Yes	1 Younger outlier
06RMG07	58.8	±1.1	3.6	±2.9	No	Simple
07RMG66	59.4	±0.6	1.3	±1.9	Yes	2 Older Cretaceous–Paleocene spots
98IB6	58.7	±0.6	1.1	±1.2	Yes	1 Older Paleocene spot
98IB12	54.8	±1.2	5	±1.6	Yes	2 Older rims; Cretaceous–Paleocene cores and mantles
98IB13	53.2	±0.8	9.5	±1.5	Yes	Cretaceous–Paleocene cores and mantles; large scatter
06RMG02	60.9	±1.0	5	±2.1	Yes	3 Cretaceous cores; 10 Ma spread in rim data
06RMG09	inconclusive				Yes	Peaks at 53 and 62 Ma
Challis intrusions						
07RMG10	50.7	±1.1	1.7	±3.8	Yes	Common Pb
06RMG05	48.4	±1.3	4.6	±3.5	No	Common Pb
98IB22	47.8	±0.7	1.4	±0.9	No	Common Pb
07RMG23	47.9	±0.7	1.7	±2.9	No	Common Pb; one Cretaceous grain
07RM G04	46.8	±0.3	2.2	±1.0	No	Common Pb
98IB24	45.6	±0.7	2.7	±2.1	No	Common Pb; one Cretaceous grain
08RMG32	44.9	±0.5	5.4	±1.0	No	Common Pb
98IB61	43.8	±0.5	1.8	±1.3	No	Common Pb
06RMG04	~50					Range of Eocene ages and numerous Cretaceous zones

[a] Uncertainty based on in-run error only

[b] MSWD based on in-run errors only

[c] Final error including uncertainty from standards

[d] Whether inherited Precambrian cores are present

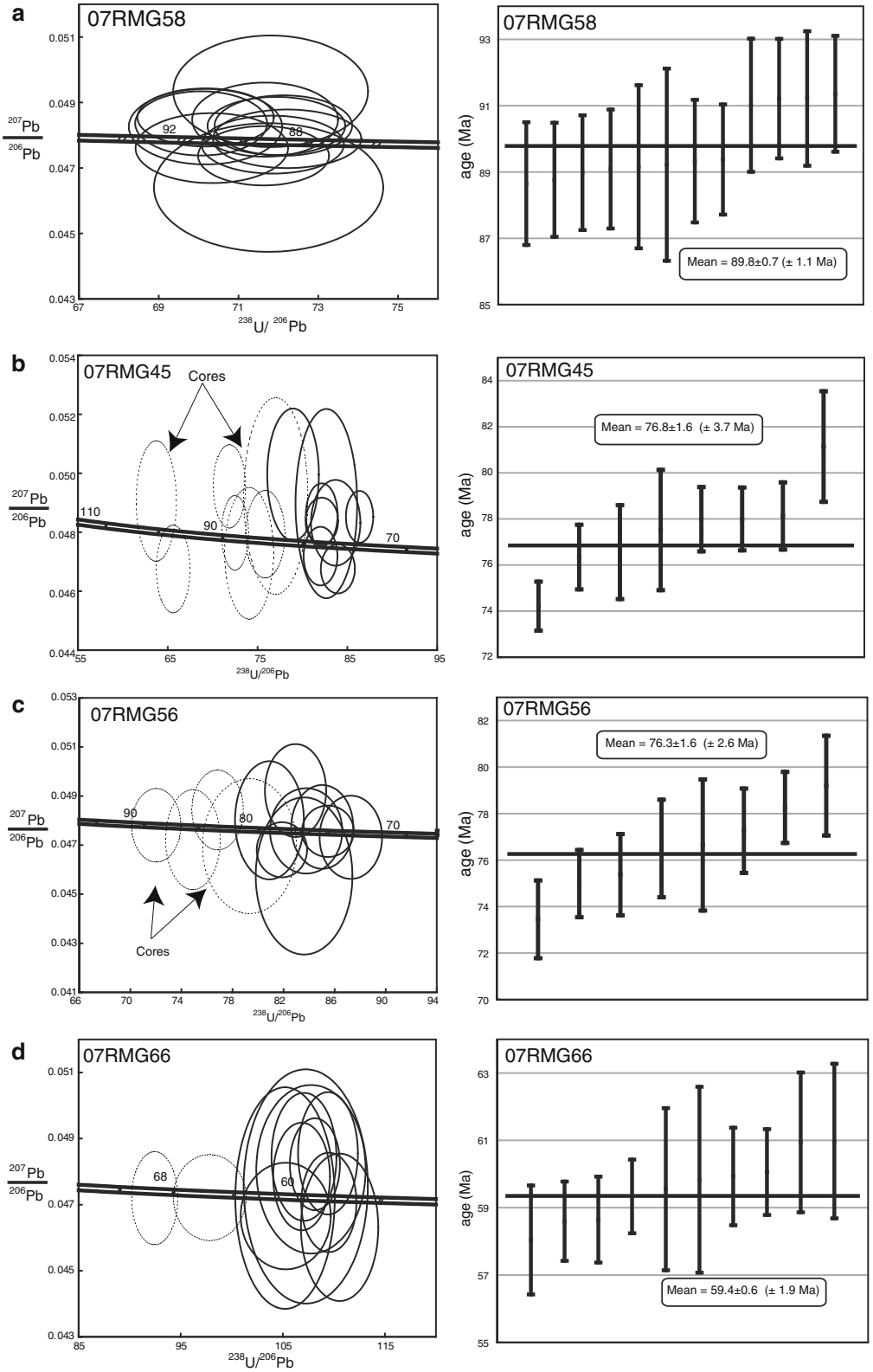

Fig. 3 Representative examples of U–Pb age systematics of zircons from different suites. Plots on the *left* are Tera–Wasserburg plots, and plots on the *right* are weighted mean $^{206}Pb/^{238}U$ age plots. *Error ellipses* with *solid outlines* in the Tera–Wasserburg plots represent analyses that are pooled for weighted mean $^{206}Pb/^{238}U$ age plots on the *right* while *dashed ellipses* are excluded. All *error ellipses* and *bars* are shown at the 2σ level. Sample 07RMG58, early metaluminous suite; 07RMG56 and 07RMG45, Atlanta peraluminous suite; 07RMG66 and 98IB12, Bitterroot peraluminous; 07RMG10 and 07RMG04, Challis intrusions

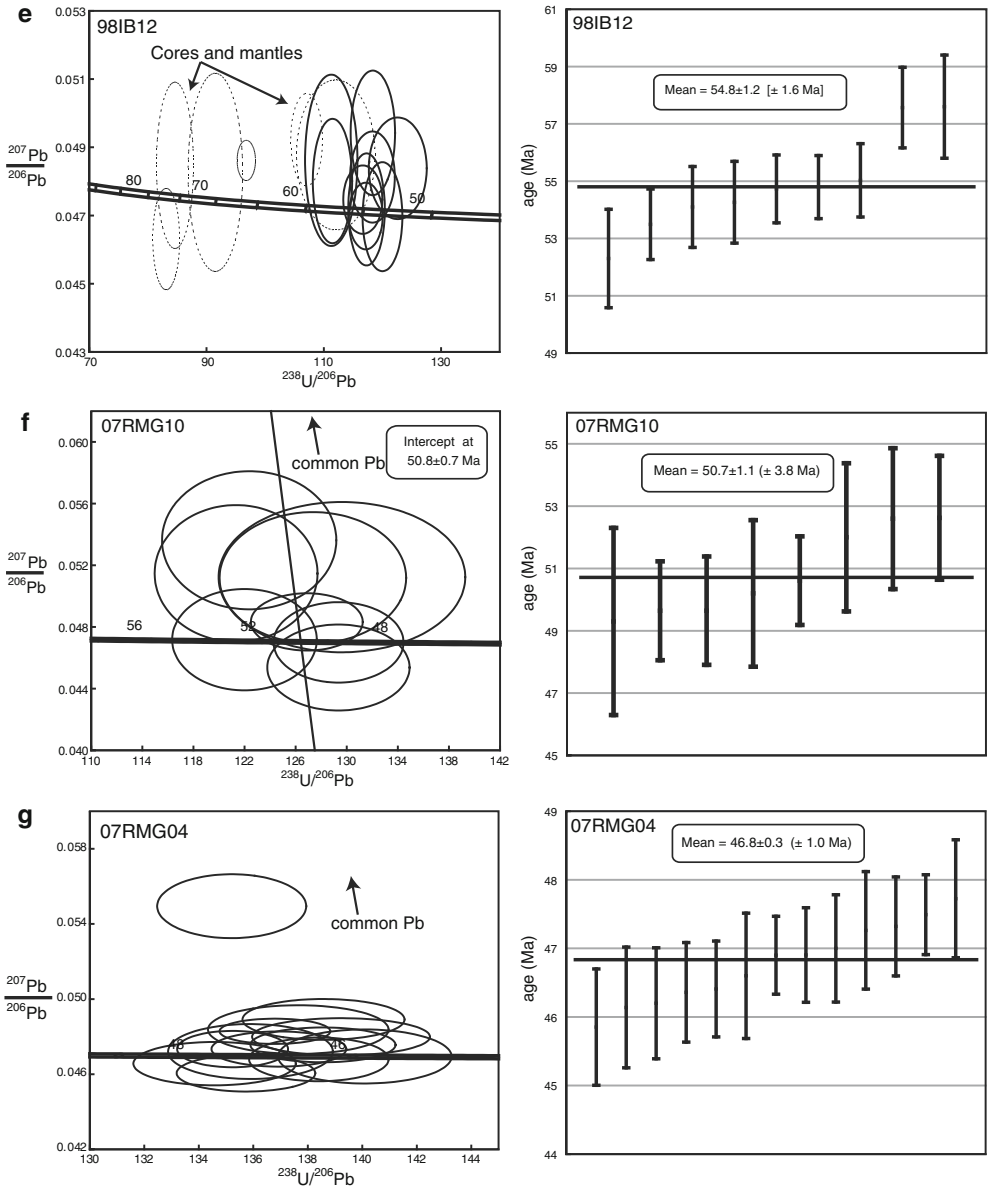

Fig. 3 continued

presented in Appendix B in ESM. Uncertainties in the isotopic ratios are reported at the 1σ level. The age is assigned based on the weighted mean of observed ^{206}Pb/^{238}U ages corrected using the ^{207}Pb correction method. Age uncertainties are reported at the 95% confidence level.

Results

Border zone suite

Only one sample of the border zone suite (98IB34) was dated in this study because of the large amount of published work on these rocks. This sample was collected from a tonalite along Slate Creek, just east of the Salmon River suture zone and the ^{87}Sr/^{86}Sr 0.706 isopleth (King et al. 2007). The majority of analyses yield an age of 85.0 ± 2.1 Ma. These rocks were presumed to be correlative with the Payette River tonalite in the McCall area to the south (Manduca et al. 1992; 1993), but our age is younger than the ages around 90 Ma obtained by both ID-TIMS and SHRIMP by Snee et al. (1995) for this same area, by Manduca et al. (1993), Giorgis et al. (2008), and Unruh et al. (2008) from McCall, and by McClelland and Oldow (2007) for equivalent rocks to the north. This suggests that plutonism just inboard of the Salmon River

suture zone and western Idaho shear zone may have been prolonged. We also observed two inherited Paleoproterozoic cores in this sample.

Early metaluminous suite

We analyzed six samples from various phases of the early metaluminous suite and these consistently yielded the oldest magmatic ages encountered in this study. These samples contain simple magmatic zircons, often with well-developed oscillatory zoning and rare inheritance (Fig. 2a). Sample 07RMG41 was collected from the Croesus quartz diorite in the southeastern corner of the Atlanta lobe and contained acicular zircons with only limited CL sector zoning, yielding an age of 98.2 ± 2.1 Ma. Samples 07RMG40 and 07RMG35, from the neighboring K-rich hornblende-bearing granodiorites to the northwest, yielded ages of 91.4 ± 2.6 and 90.9 ± 1.8 Ma, respectively. Sample 07RMG36 was collected from a hornblende–biotite tonalite occurring as a roof pendant within the peraluminous main phases of the Atlanta lobe along the South Fork of the Boise River and yielded an age of 86.7 ± 2.8 Ma.

Two samples of the distinctive porphyritic granodiorite described above were studied. Sample 07RMG58 (Fig. 3a) was collected from this unit east of Stanley at the same outcrop dated by Lewis et al. (1987) using ID-TIMS. We obtained a LA-ICP-MS age of 89.8 ± 1.1 Ma, indistinguishable from the age of 88 ± 6 reported by Lewis et al. (1987). Sample 99RL293 was collected from Red River Hot Springs, near Elk City in north-central Idaho and dated by SHRIMP-RG. Aside from two Mesoproterozoic cores, core and rim domains give $^{206}Pb/^{238}U$ ages ranging from 95 to 91 Ma. Assuming the two ca. 95 Ma domains reflect the effects of inherited components, the remaining analyses give a weighted mean $^{206}Pb/^{238}U$ of 92.4 ± 0.8 Ma, which is interpreted as the crystallization age of the sample.

Atlanta peraluminous suite

We analyzed seven samples (98IB68, 07RMG25, 07RMG28, 07RMG29, 07RMG45, 07RMG46, 07RMG56) of the voluminous biotite granodiorite phase of the Atlanta peraluminous suite. Zircons from these samples display a variety of morphologies, including a distinct subpopulation of spindle-like crystals dominated by long, prominent pyramidal terminations. In CL, zircons generally consist of bright cores surrounded by dark rims (Fig. 2c, d). The bright cores are indicators of pervasive inheritance in these samples, and this inheritance can be divided into two categories. All but one of the samples contains zircons with Precambrian cores, predominantly of either Neoproterozoic or late Archean age. In addition, every sample contains multiple generations of Cretaceous zircon growth. In all cases, the youngest generation is the most widespread, which we interpret to represent the sample crystallization age, but a few analyses yield ages that are 10–15 Ma older than the dominant age. While these older Cretaceous ages commonly come from zircon cores, they have also been observed as rims surrounding Precambrian cores and mantles between Precambrian cores and still younger rims. There is no systematic relationship in the individual samples between the different Cretaceous age populations and Th/U ratios, which are sometimes used to differentiate between magmatic and metamorphic or hydrothermal zircon (Hoskin and Schaltegger 2003). It is important to note that the older Cretaceous ages typically overlap with the age range of the early metaluminous suite quoted above.

Our interpreted crystallization ages for samples of the biotite granodiorite phase of the Atlanta peraluminous suite range from 83 to 68 Ma. Although there are no definitive spatial patterns, the oldest sample (98IB68) is the easternmost and is intimately associated with the porphyritic granodiorite near Stanley, and the two youngest samples are the southernmost, collected between Atlanta and Rocky Bar.

The Atlanta lobe is cored by bodies of muscovite–biotite granite that generally show diffuse contacts with the surrounding biotite granodiorite. We studied two samples of this phase (07RMG52 and 98IB53), both from the central Atlanta lobe. Both samples are characterized by bright CL cores with fine-scale zoning surrounded by very dark CL rims (Fig. 2d). In the case of 07RMG52, the majority of the cores give ages indistinguishable from the rims, yielding a weighted mean of 80.2 ± 1.5 Ma, similar to results reported by Unruh et al. (2008) for muscovite–biotite granite samples in the northern Atlanta lobe. In the case of 98IB53, these cores represent the same kind of complex inheritance seen in biotite granodiorite samples, where some cores yield Proterozoic ages and some yield only slightly older Cretaceous ones. The weighted mean of the rim ages from this sample is 74.6 ± 1.7 Ma.

We studied one sample (07RMG43) of the leucogranite phase that generally occurs as isolated dike-like masses in the Atlanta lobe. This sample, collected near the settlement of Grandjean, was unique in that in addition to containing normal-sized euhedral zircons, it also contained several large zircon fragments consisting almost entirely of inherited domains with a uniform age of ~670 Ma and only very narrow Cretaceous overgrowths (Gaschnig et al. 2008). The smaller euhedral grains also contained cores with this Neoproterozoic age but generally with larger rims. The rims ages yield a weighted mean of 71.2 ± 2.0 Ma.

We also collected a biotite–muscovite granite sample from the Moscow Mountain pluton, an Idaho batholith outlier north of Moscow, in order to determine whether it is a portion of the Bitterroot peraluminous suite or a northern

extension of the Atlanta peraluminous suite. Zircon rims yield a bimodal age distribution, centered at 79 and 75 Ma. Consequently, the exact crystallization age of the rock is uncertain but it is clearly late Cretaceous and consistent with being correlative with the Atlanta peraluminous suite.

Late metaluminous suite

Three samples were collected from the late metaluminous suite, which forms a discontinuous envelope of intrusions surrounding the peraluminous interior of the Bitterroot lobe. A quartz diorite sample (01RL700) was collected from the western side of this suite near the town of Headquarters. It contained zircons with sector and weak concentric zoning. A small number of grains contained distinct CL cores. Many of these have ages indistinguishable from their rims, but a few give Paleoproterozoic ages. The rims show some effects of common Pb and yield a weighted mean age of 73.1 ± 3.7 Ma.

Sample 01RL729, from the northern portion of this suite, was collected from a biotite-rich and hornblende-bearing granodiorite originally considered part of the Eocene Lolo batholith but now mapped as the Toboggan Ridge stock, a separate body (Lewis et al. 2007b). Zircons from sample 01RL729 display oscillatory zoning patterns (Fig. 2b) similar to the early metaluminous suite, and only a few dark CL cores are present, which yield Paleoproterozoic ages. The simple grains and rims of complex grains yield a weighted mean age of 71.3 ± 1.6 Ma.

A quartz diorite sample (06RMG01) was collected from the southern end of the same large pluton where sample 01RL600 was collected, and its zircons exhibit the same characteristics as 01RL600. In the case of 06RMG01, however, the zircon rims yield a slightly younger weighted mean age of 68.9 ± 2.8 Ma.

Bitterroot peraluminous suite

We studied 11 samples of the Bitterroot peraluminous suite. Seven of these (06RMG03, 06RMG07, 06RMG08, 06RMG09, 07RMG04 98IB6, and 98IB12) were collected from along the Lochsa River, and the other samples were collected from Lolo Creek (06RMG02), Lolo Trail (07RMG66), Tom Beal Park (07RMG70), and Lost Horse Canyon (98IB13). Most of these samples contain a subpopulation of zircons that display a very distinct spindle-like morphology, characterized by prominent long, sharp pyramidal terminations. CL-imaging reveals distinct cores in the majority of grains (Fig. 2e, f). The U–Pb systematics are also very complex for nearly all samples. Like the peraluminous Atlanta lobe samples, most of these samples contain both multiple Precambrian (Mesoproterozoic through Archean) cores and Late Cretaceous components but, unlike the Atlanta lobe, are dominated by Paleocene rim ages. In addition, numerous zircons were found displaying a complex record of growth with Proterozoic cores, Cretaceous mantles, and Paleocene rims (e.g., Fig. 2f).

The zircon rims in the majority of samples give a narrow range of ages between ~62 and 58 Ma, although ages as old as 65.9 ± 3.5 Ma and as young as 53.2 ± 1.5 Ma were also obtained. No systematic relationship between age and location was apparent.

Several samples deserve special mention. The oldest sample from this suite with the oldest crystallization age (07RMG70) came from a texturally distinct and spatially limited subunit located in Tom Beal Park, south of the Lochsa River. This sample is characterized by prominent muscovite phenocrysts and yielded a weighted mean age of 65.9 ± 3.5 Ma. Sample 98IB6, which came from an outcrop complex containing a mafic dike dated by Foster and Fanning (1997) using the Ar–Ar method on hornblende, yielded an age of 58.7 ± 1.2 Ma, which overlaps with their age of 56.5 ± 1.7 Ma. These ages provide some support for Foster and Hyndman's (1990) assertion that the intrusion of mafic dikes along the Lochsa corridor was coeval with the main phase of granitic magmatism, although additional data presented below suggests that other mafic rocks they describe may be Eocene and related to Challis magmatism. Two samples (06RMG03 and 98IB12) with disparate ages, well beyond the limits of precision and accuracy of the LA-ICP-MS method, came from the same general location in the Black Canyon segment of the Lochsa River, near the western edge of the Bitterroot lobe. Sample 06RMG03, a biotite–muscovite granodiorite with variable muscovite abundance, yielded an age of 65.6 ± 3.6 Ma. Sample 98IB12 (Fig. 3e), which yielded an age of 54. 8 ± 1.6 Ma, was collected a few hundred meters to the southwest from a sheet-like mass of granite in a complex zone of steeply dipping and partially migmatized metasedimentary wallrock screens. The granite itself, although superficially similar to 06RMG03, is slightly coarser overall with less muscovite and shows broad feldspar zoning in thin section, which is commonly absent in the Bitterroot peraluminous suite.

We also analyzed zircons from a hybrid diorite phase (07RMG04; Fig. 3f) in order to directly test the hypothesis of Hyndman (1984), Hyndman and Foster (1988), and Foster and Hyndman (1990) that a significant amount of mafic magmatism in the Bitterroot lobe is co-magmatic with the main (Paleocene) peraluminous biotite granodiorite phase. This sample came from a mafic complex along the Lochsa River at Bald Mountain Creek, described in detail by Williams (1977) and Hyndman (1984) and among the largest of several such complexes in the Bitterroot lobe. The sample contained abundant acicular, inclusion-rich zircons with patchy CL zoning that yielded an age of

46.8 ± 1.0 Ma with no inheritance. This suggests that, in spite of the similarity between Foster and Fanning's (1997) mafic dike age and our Paleocene host granodiorite sample (98IB6), a significant portion of the mafic magmatism described by Foster and Hyndman (1990) may be Eocene in age and related to the large number of Challis intrusions recently recognized in the Bitterroot lobe by Lewis et al. (2007a, b), rather than being features of the Idaho batholith proper.

One sample, 06RMG09, lacked enough large zircons to identify a definitive magmatic age due to ages complexities. The small number of zircon rims wide enough to analyze form a diffuse cluster in of latest Paleocene and early Eocene ages (ca. 55–50 Ma), whereas mantles and non-Precambrian cores cluster around 60 Ma.

Challis intrusions

We analyzed seven samples from six major Challis intrusions and one dike, all intruding older rocks of the Idaho batholith proper. Zircons from all but one of these samples were almost completely devoid of inherited components and commonly displayed either sector zoning or no zoning of any kind (Fig. 2g, h). Zircons from the quartz monzodiorite suite were typically more equant (Fig. 2h) whereas zircons from the pink granite suite were commonly acicular with abundant inclusions and apparent void spaces (Fig. 2g). U–Pb systematics for all samples show evidence of common Pb. This may be due in part to the presence of inclusions, but may also be the result of the lower levels of radiogenic Pb in these zircons due either to their younger age or low levels of U, which result in a proportionally larger contribution of common Pb in the analysis.

Challis samples yielded ages between 51 and 43 Ma. The youngest sample, 98IB6, comes from the Sheep Creek batholith, which is a large mass of pink granite along the Boise River. Its age of 43.8 ± 1.3 Ma places it near the end of Challis magmatic activity established by K–Ar and Ar–Ar geochronology (Fisher et al. 1992). It is also significantly younger than the neighboring Thorn Creek stock of quartz monzodiorite, which yielded an age of 47.9 ± 2.9 Ma (07RMG23). This is consistent with field observations that have suggested the pink granite intrusions are typically younger than quartz monzodiorite intrusions in a given locality (Lewis and Kiilsgaard 1991; Schmidt 1994; Mitchell 1997; Reppe 1997; Robertson 1997).

Sample 06RMG04 failed to yield a conclusive age. This sample, a fine-grained biotite granodiorite, was collected from the same outcrop as sample 06RMG05, a hornblende–biotite syenite, which yielded an unambiguous Eocene age of 48.4 ± 3.5 Ma, but the contact relationship between the two phases is unclear due to the deep weathering seen in the outcrop. Although the cluster of ages between 50 and 46 Ma for 06RMG04 suggests an Eocene crystallization age, the large scattering of older ages coupled with the proximity to the syenite suggest that these ages also could represent growth or recrystallization during contact metamorphism.

Discussion

The data presented here provide the first U–Pb age constraints on large portions of the Atlanta lobe of the Idaho batholith and, together with other recent contributions (e.g., Unruh et al. 2008; Giorgis et al. 2008), provide a more complete working chronology for the construction of the batholith as a whole (Fig. 4). These data establish unambiguously that the voluminous peraluminous main phases of the two lobes of the batholith, although similar in terms of petrography and major and trace element geochemistry, represent two temporally distinct episodes of magmatism. Using the data presented here, in conjunction with existing data from the literature, we construct a timeline (Fig. 5) of plutonism for the greater Idaho batholith system and compare its history to the larger Cordilleran framework.

History of the Idaho batholith

The construction of the Idaho batholith was preceded by the accretion of the Blue Mountains province to North America between about 130 and 125 Ma (Selverstone et al. 1992; Getty et al. 1993; Snee et al. 2007). The resulting Salmon River suture zone was initially stitched by the intrusion of numerous relatively small dioritic to tonalitic plutons of the suture zone suite along its length between 125 and 105 Ma (Manduca et al. 1993; Lee 2004; Snee et al. 2007; McClelland and Oldow 2007; Giorgis et al. 2008; Unruh et al. 2008). These rocks were subsequently deformed by transpressional shear on the Western Idaho shear zone, a distinct mylonite zone within the Salmon River suture zone (e.g., McClelland et al. 2000; Giorgis et al. 2008) and the suture zone suite may have been severely attenuated from a much greater original width by vertical extrusion (Giorgis et al. 2005).

Idaho batholith magmatism commenced with the formation of the early metaluminous suite, beginning with the emplacement of the Croesus stock in the southeastern Atlanta lobe at 98 Ma. This suite continued to develop with the emplacement of megacrystic granites around Elk City and along the western and eastern margins of the Bitterroot lobe at 95 Ma (Lund et al. 2008; personal communication) and between 93 and 90 Ma to the south (Unruh et al. 2008, this paper). Equigranular granodiorites and tonalites of this suite were emplaced between 93 and 87 Ma in the southeastern corner of the Atlanta lobe.

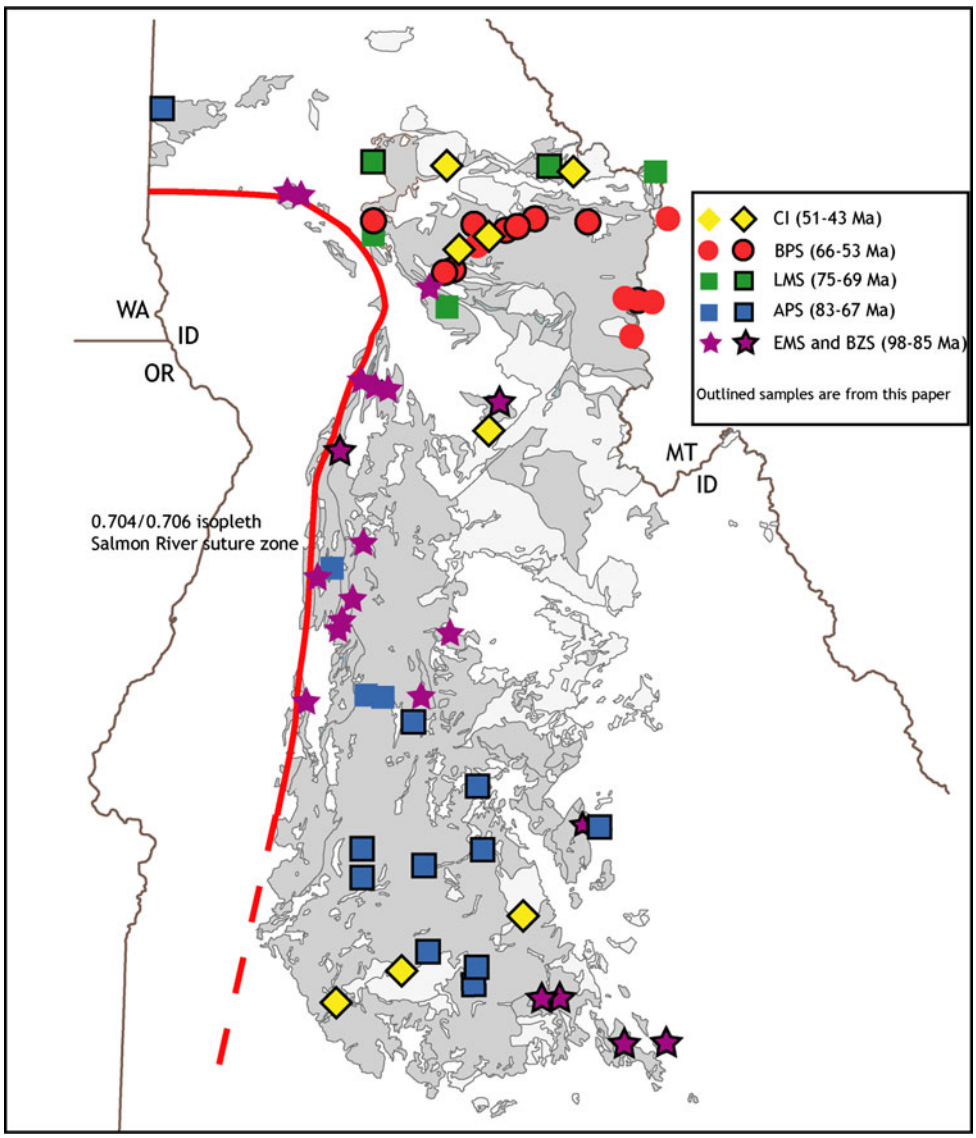

Fig. 4 Summary map of Idaho batholith (*dark gray*) and Challis intrusions (*light gray*) showing the ages presented in this paper (*outlined symbols*) and the other in situ dates from the literature (Foster and Fanning 1997; Foster et al. 2001; Lee 2004; Foster et al. 2007a; McClelland and Oldow 2007; Giorgis et al. 2008; Lund et al. 2008). Samples with concordant, overlapping ages from the ID-TIMS dataset of Unruh et al. (2008) are also shown

Starting around 90 Ma and probably continuing for several million years, tonalitic sheet-like plutons of the border zone suite were emplaced adjacent to the suture zone (Manduca et al. 1993; Lee 2004; McClelland and Oldow 2007; Giorgis et al. 2008; Unruh et al. 2008). The similarity in age and chemistry between the early metaluminous suite and the border zone suite suggests to us the possibility that they represent the remnants of a much larger contiguous Late Cretaceous igneous system that was dismembered by subsequent episodes of plutonism. Plutons of this age are also present in the Idaho Panhandle region and adjacent northeastern Washington, forming parts of the Kaniksu batholith (Archibald et al. 1984; Whitehouse et al. 1992; Miller et al. 1999; R. M. Gaschnig, unpublished data), which would extend the length of this system to almost 600 km.

The voluminous Atlanta peraluminous suite was constructed between 83 and 67 Ma and represents the largest single component of the Idaho batholith, roughly twice the cumulative area of all the other suites of the batholith (excluding the Challis intrusions). This interval also has the greatest rate of magmatism in the formation of the batholith, with an apparent magmatic flux of $\sim$1,000 km^2/Ma, roughly three times that of the combined border zone and early metaluminous suites. Although it is difficult to make strong assertions about time–space patterns within the suite due to our modest number of samples compared to the vast size of the Atlanta lobe, our data broadly indicate that both the biotite granodiorite and muscovite–biotite granite phases are generally older in the northern and eastern parts of the suite. This is supported by TIMS zircon U–Pb data presented by Unruh et al. (2008) for the several samples of

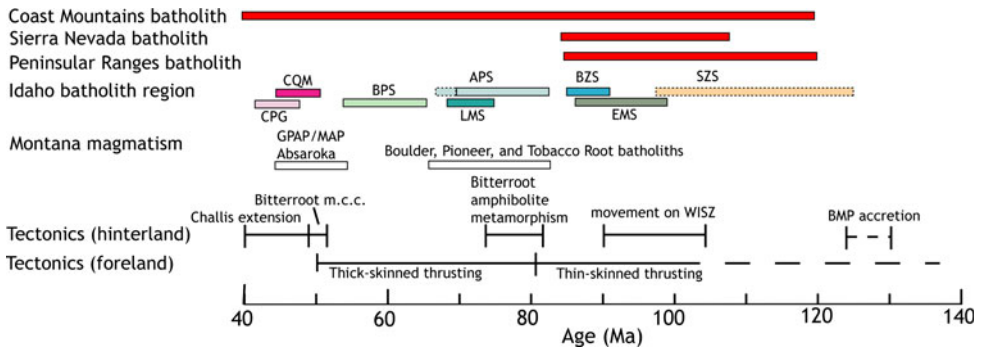

Fig. 5 Schematic *time line* showing major episodes of magmatism in the greater Idaho batholith system, along with other events in the Cordillera. The outline of the suture zone suite is *dashed* because the relative paucity of data makes it unclear whether magmatism was continuous or sporadic during that interval. Sources not mentioned in the text of the paper for ages of other provinces are: Bateman (1992), Coleman and Glazner (1997), Duke (2009), Feeley (2003), Friedman and Armstrong (1995), Gehrels et al. (2009), Ortega-Rivera et al. (1997), Ortega-Rivera (2003) , and Saleeby et al. (2008). *APS* Atlanta peraluminous suite, *BB* Boulder batholith, *BMP* Blue Mountains Province, *BPS* Bitterroot peraluminous suite, *BZS* border zone suite, *CPG* Challis pink granite suite, *CQM* Challis quartz monzodiorite suite, *EMS* early metaluminous suite, *GPAP/MAP* Great Plains alkalic province/Montana alkalic province, *LMS* late metaluminous suite, *MCC* metamorphic core complex, *PB* Pioneer batholith, *SZS* suture zone suite, *TB* Tobacco Root batholith, *WISZ* Western Idaho shear zone

the northern Atlanta peraluminous suite which, although widely dispersed along concordia due to the complexity of the zircons, suggested ages between 85 and 75 Ma.

Our two southernmost samples of biotite granodiorite, 07RMG28 and 07RMG29, yield distinctly younger ages (~68 Ma) than the rest of the Atlanta peraluminous suite. These rocks appear to represent a limited "last gasp" of magmatism in the southern Atlanta lobe, which may have important metallogenic significance due to their proximity and age equivalence to the nearby Atlanta gold deposits (Snee and Kunk 1989). They also may be related to the aplite–pegmatite dike complex at the Atlanta lobe's southern margin, which has an approximate age of 66 Ma (Alexander et al. 2006).

The vast majority of the Atlanta peraluminous suite, based on the existing geochronology and new data presented here, occurs within the Atlanta lobe as traditionally defined. One conspicuous exception to this is shown by the Moscow Mountain (09RMG01) sample, which, by virtue of its age and composition, is most closely related to the Atlanta peraluminous suite despite its northern location.

A second, more localized, episode of metaluminous magmatism, producing the late metaluminous suite, began around 76 Ma (Foster et al. 2001) with the emplacement of the Skookum Butte pluton in the northeastern corner of the Bitterroot lobe. The Toboggan Ridge stock was emplaced slightly later around 71 Ma. A large body of quartz diorite was also emplaced on the west side of the Bitterroot between 73 and 69 Ma (McClelland and Oldow 2007, this paper). Similar rocks are also present near the southern edge of the Bitterroot lobe but were not studied here. The development of the late metaluminous suite appears to be coeval with amphibolite facies metamorphism in the wallrocks northeast of the Bitterroot lobe (House et al. 1997).

The late metaluminous magmatism in the northern Idaho batholith was followed by the formation of the Bitterroot peraluminous suite. Peraluminous magmatism began around 66 Ma and peaked around 60 Ma. The mafic magmatism in the Bitterroot lobe described by Hyndman and Foster (1988) and Foster and Hyndman (1990) apparently commenced by ~58 Ma (Foster and Fanning 1997, this paper) and continued into the Eocene, producing many mafic dikes, sills, and small intrusive complexes. The peraluminous magmatism continued until about 53 Ma. This last phase of magmatism was originally thought to be only localized in the Bitterroot Mountains (Foster and Fanning 1997; Foster et al. 2001; Foster et al. 2007a), but our age for sample 98IB-12 in the western Bitterroot lobe suggests it might have been more widespread. Local migmatite formation also occurred as late as ~53 Ma in the Bitterroot Mountains (Foster et al. 2001). As a whole, this pulse of Bitterroot peraluminous magmatism only produced an area roughly one quarter of the size of the Atlanta peraluminous suite, with an apparent flux only one-third as great.

Magmatism in the Idaho batholith proper (98–53 Ma) essentially followed a cyclic pattern, consisting of two cycles that each began with low volume, compositionally diverse, metaluminous magmatism and were followed by high volume, compositionally restricted, peraluminous magmatism. The first cycle lasted from 98 to 67 Ma and led to the construction of the early metaluminous, border zone, and Atlanta peraluminous suites. The second episode

was more spatially restricted and lasted from 75 to 53 Ma, leading to the construction of the late metaluminous and Bitterroot peraluminous suites. These cycles may be a product of episodic crustal thickening. Similar cyclic patterns between magmatic flux and crustal input have also been observed in the Coast Mountains and Sierra Nevada batholiths as well as in the central Andes (DeCelles et al. 2009).

All phases of the Idaho batholith were subsequently cut by the dikes and plutons of the Challis magmatic event, which began around 52 Ma in response to crustal extension and also led to widespread volcanism in Idaho and neighboring states. This was coincident with the formation of the Bitterroot mylonite, the exhumation of the Bitterroot metamorphic core complex (e.g., Foster and Fanning 1997; Foster et al. 2001), and development of a system of northeast-trending faults and grabens (e.g., Janecke 1992; Janecke et al. 1997). Challis volcanism and plutonism proceeded simultaneously. Geochronology presented here and elsewhere (Armstrong 1974; Criss et al. 1982; Fisher et al. 1992; Foster et al. 2001; House et al. 2002) indicates that plutonism began around 51 Ma, peaked between 48 and 46 Ma, and lasted until about 43 Ma, with an apparent magmatic flux roughly equal to the Atlanta peraluminous suite (and much greater if the volcanic rocks are also considered). In a given area, emplacement of plutons of the quartz monzodiorite suite generally preceded emplacement of the pink granite suite. Overall, the cessation of plutonism and dike emplacement (Simonsen 1997), appears to have occurred progressively from north to south. The volcanic record of the Challis event, preserved in southeastern Idaho, appears to parallel the compositional and temporal trends of the intrusions, with an initial phase dominated by mafic-to-intermediate effusive lavas followed by a short hiatus and a second predominantly explosive, silicic caldera-forming phase (Fisher et al. 1992; Janecke and Snee 1993; McKervey 1998). This similarity has led to the proposal that the effusive lavas are erupted equivalents of the quartz monzodiorite suite and the explosive silicic volcanic rocks are the erupted equivalent of the pink granite suite (Lewis and Kiilsgaard 1991; McKervey 1998). Additional and more precise geochronology on both the volcanic and intrusive rocks is needed in order to evaluate this hypothesis.

Larger framework

Figure 5 displays a timeline of different phases of Idaho batholith magmatism in the context of the other batholiths of the Cordillera and regional tectonics. The most striking observation is the relatively short and focused nature of activity in the Sierra Nevada and Peninsular Ranges batholiths in the Late Cretaceous compared to the Idaho and Coast Mountains batholiths. While the border zone and early metaluminous suites were coeval with the Late Cretaceous flare-ups in the Sierra Nevada and Peninsular Ranges batholiths, the bulk of the Idaho batholith was constructed after this interval. The cessation of magmatism in the two southern batholiths by 80 Ma and concurrent change in deformational style from thin to thick-skinned thrusting (e.g., Dickinson et al. 1988; DeCelles 2004), traditionally attributed to the shallowing of the dip of the subducting Farallon slab (e.g., Saleeby 2003), was coincident with the initiation of the voluminous Atlanta peraluminous magmatism. Magmatism also spread into southwestern Montana around this time, leading to the formation of numerous satellite batholiths and plutons. These were intruded at shallow levels in the crust, dominated by metaluminous compositions, and include the Boulder batholith (80–74 Ma; Lund et al. 2002), Pioneer batholith (75–72 Ma; Murphy et al. 2002), and Tobacco Root batholith (77–75 Ma; Mueller et al. 1996; Cheney et al. 2004). These batholiths also generally follow the trend of the Great Falls tectonic zone, a Precambrian structure separating the Archean Wyoming and Hearne provinces. Foster et al. (2006, 2007b) attributed this to an intrinsic fertility in the lower crust along this structure, with melting possibly induced by asthenospheric flow around a tear or fracture in the subducting slab between a segment to the north with a normal dip and segment to the south with a shallow dip.

The more spatially restricted nature of the second peraluminous pulse in the Idaho batholith, leading to the formation of the Bitterroot peraluminous suite, is a curious feature but is in many ways analogous to the mid-crustal migmatization and peraluminous magmatism in metamorphic core complexes in Canada and northern Washington (Sevigny et al. 1989; Carr 1992; Vanderhaeghe et al. 1999; Hinchey et al. 2006; Gordon et al. 2008; Kruckenberg et al. 2008). The localized nature of this suite may be the result of more focused crustal thickening in this specific area, consistent with the recent work of Lund et al. (2008).

As a whole, the magmatic record provided by the Idaho batholith has much more in common temporally with the Coast Mountains batholith than the Sierra Nevada or Peninsular Ranges batholiths but the relationship between composition, space and time in the Idaho batholith are relatively unique. All three of the other batholiths are dominantly metaluminous and consist broadly of older, more mafic western belts and younger, more felsic eastern belts, separated either by major structures or gradational boundaries (e.g., Bateman 1992; Tulloch and Kimbrough 2003; Crawford et al. 2005; Gehrels et al. 2009). In contrast, the distinct temporal and compositional belts of Idaho batholith largely overlap in space and evolved peraluminous rocks comprise the largest fraction of its volume. The

peraluminous character undoubtedly relates at least in part to the construction of the Idaho batholith entirely in Precambrian continental crust, in contrast to the other three Cordilleran batholiths.

Significance of Cretaceous inheritance

The implications of inherited Precambrian cores for the terrane architecture and Precambrian history of the region are beyond the scope of this paper, but the significance of the inherited Cretaceous cores and mantles deserve mention because it has implications for the earlier history of the batholith. The presence of zircons with a spread of pre-eruption ages in volcanic rocks has recently received a great deal of attention (e.g., Reid et al. 1997; Bindeman et al. 2001; Vazquez and Reid 2002; Simon and Reid 2005; Simon et al. 2008), and a similar phenomenon has been observed in some plutonic systems (Coleman et al. 2004; Walker et al. 2007; Miller et al. 2007). These typically reflect age differences on the scale of tens of thousands to a few million years, and the smear that we see along concordia for zircon rim ages in our samples may be an analogous phenomenon, reflecting magmatic recharge and further complicated by Pb loss. However, we also see within-sample core–rim variations as great as 25 million years. Recycling of zircons on this timescale has been previously documented in the Bitterroot lobe of the Idaho batholith by Foster and Fanning (1997) and Foster et al. (2001) and recently in other plutonic localities (e.g., Bolhar et al. 2008).

Nearly all of our samples from the Atlanta peraluminous suite contain Cretaceous cores and/or mantles with age ranges coincident with the early metaluminous suite (~100 to 85 Ma). Although the metaluminous suite is exposed most prominently along the eastern edge of the Atlanta lobe, plutons correlative with this suite also occur as apparent roof pendants within the peraluminous suite. These two points suggest to us that the early metaluminous suite was originally more extensive, covering a much greater area and possibly even connecting laterally with the coeval border zone suite. One possible scenario is that these intrusions were emplaced at a higher structural level in the crust than the later peraluminous magmas and most were subsequently eroded away. The roof pendant relationship seen in parts of the Atlanta lobe seems to support this, along with Al-in-hornblende thermobarometry from metaluminous plutons in the Hailey area indicating upper-mid crustal emplacement levels of ~3 to 4 kbars (Jordan 1994). In this scenario, zircon inheritance in the peraluminous granitoids would come either from limited wall-rock assimilation at their emplacement level or remelting of residual metaluminous melts in their source region or in fossil magma conduits. Another possibility is that the metaluminous suite was assimilated by the subsequent invading peraluminous magmas at the same level of emplacement, leaving only the limited remains that we observe today. The absence of large quantities of granitic xenoliths and inherent thermal limitations on assimilation (e.g., Glazner 2007), however, make this a less likely explanation in our opinion.

A particularly interesting example of apparent pluton recycling or cannibalization from the Atlanta lobe is seen in the youngest (~67 Ma) and southernmost samples from the Atlanta peraluminous suite (07RMG28 and 07RMG29). Both of these samples contain cores and mantles with ages consistent with the metaluminous suite, but they also contain isolated age elements components between 80 and 70 Ma, which is the interval during which the bulk of the Atlanta peraluminous suite was constructed.

The zircons from the Bitterroot peraluminous suite also exhibit Cretaceous inheritance but in this case, most of these ages fall between 80 and 70 Ma. Although this age range corresponds to the main pulse of magmatism in the Atlanta peraluminous suite, it also corresponds, at least in part, to the formation of the late metaluminous suite. Since these rocks form a kind of envelope surrounding much of the Bitterroot peraluminous suite, they may be equivalent to the source of the inherited zircon.

Conclusions

New in situ LA-ICP-MS U–Pb zircon geochronology, coupled with other recent and ongoing studies, help to define a long and complex history of magmatism in the Idaho batholith system. This magmatism occurred as two cycles consisting of low volume metaluminous magmatism followed by high volume peraluminous magmatism, prior to the Challis magmatic event. Following the accretion of the Blue Mountains province around 125 Ma and sporadic plutonism in the resulting suture zone, Idaho batholith magmatism commenced around 98 Ma with the emplacement of metaluminous magmas into Precambrian North American crust well east of the suture zone. A second parallel metaluminous belt, the border zone suite, developed adjacent to the suture zone around 90 Ma and magmatism continued in both belts until about 85 Ma. Starting around 80 Ma, plutonism became more voluminous and predominantly peraluminous, most likely in response to thickening of the crust, leading to the formation of the vast Atlanta peraluminous suite. Also at about this time, a northeast-trending belt of metaluminous satellite plutons and batholiths began to form in western Montana and metaluminous forerunners of the Bitterroot lobe of the Idaho batholith were also emplaced. Localized Atlanta lobe peraluminous magmatism occurred as late as 67 Ma, but

activity in the Atlanta lobe had largely ceased by the time Bitterroot peraluminous magmatism began to the north at 66 Ma. The bulk of the Bitterroot peraluminous suite was constructed around 60 Ma, but voluminous plutonism and localized migmatization continued until as late as 53 Ma, nearly overlapping with the subsequent Challis magmatic event. The Challis event included both volcanism and plutonism and occurred in two distinct pulses during the Eocene, leading to the formation of distinct plutonic and volcanic suites. Zircon inheritance is pervasive in the peraluminous phases of the batholith, and consists of both Precambrian and slightly older ($\sim$10 to 20 million years) components, the latter apparently reflecting the reworking of earlier phases of the batholith.

Acknowledgments We would like to acknowledge support from NSF grants EAR-0537913 and EAR-0844149, a Geological Society of America Graduate Student Research Grant, and Praetorius-Exxon Graduate Fellowship from WSU. We thank Charles Knaack and Paul Olin for analytical help with LA-ICPMS. We also greatly appreciate the zircon separates provided by Elizabeth King and John Valley. We also would like to thank Mary Reid and an anonymous reviewer for their constructive and helpful comments.

References

Alexander JT, Schmitz MD, Northrup CJ (2006) Preliminary U/Pb zircon data from the House Mountain metamorphic complex in the Atlanta lobe of the Idaho batholith. Geol Soc Am Abstr Programs 38(7):483

Archibald DA, Krogh TE, Armstrong RL, Farrar E (1984) Geochronology and tectonic implications of magmatism and metamorphism, southern Kootenay Arc and neighboring regions, southeastern British Columbia. Part II: mid-Cretaceous to Eocene. Can J Earth Sci 21:567–583

Armstrong RL (1974) Geochronometry of the Eocene volcanic-plutonic episode in Idaho. Northwest Geol 3:1–15

Armstrong RL (1975a) The geochronometry of Idaho. Isochron/West 14:1–50

Armstrong RL (1975b) Precambrian (1500 m.y. old) rocks of central Idaho—the Salmon River Arch and its role in Cordilleran sedimentation and tectonics. Am J Sci 275-A:437–467

Armstrong RL (1988) Mesozoic and early Cenozoic magmatic evolution of the Canadian Cordillera. In: Burchfiel BC, Suppe J (eds) Processes in continental lithospheric deformation. Geol Soc Am Spec Pap 218:55–92

Armstrong RL, Taubeneck WH, Hales PO (1977) Rb-Sr and K-Ar geochronometry of Mesozoic granitic rocks and their Sr isotopic composition, Oregon, Washington, and Idaho. Geol Soc Am Bull 88:397–411

Barth AP, Wooden JL, Coleman DS (2001) SHRIMP-RG U-Pb zircon geochronology of Mesoproterozoic metamorphism and plutonism in the southwesternmost United States. J Geol 109:319–327

Bateman PC (1992) Plutonism in the central part of the Sierra Nevada batholith. U.S. Geological Survey Professional Paper 1483, 186 p

Bickford ME, Chase RB, Nelson BK, Shuster RD, Arruda EC (1981) U-Pb studies of zircon cores and overgrowths, and monazite; implications for age and petrogenesis of the northeastern Idaho batholith. J Geol 89(4):433–457

Bindeman IN, Valley JW, Wooden JL, Persing HM (2001) Post-caldera volcanism; in situ measurement of U-Pb age and oxygen isotope ratio in Pleistocene zircons from Yellowstone Caldera. Earth Planet Sci Lett 189:197–206

Black LP, Kamo SL, Allen CM, Davis DW, Aleinikoff JN, Valley JW, Mundil R, Campbell IH, Korsch RJ, Williams IS, Foudoulis C (2004) Improved 206Pb/238U microprobe geochronology by the monitoring of a trace-element-related matrix effect; SHRIMP, ID-TIMS, ELA-ICP-MS and oxygen isotope documentation for a series of zircon standards. Chem Geol 205(1–2):115–140

Bolhar R, Weaver S, Palin J, Cole J, Paterson L (2008) Systematics of zircon crystallisation in the Cretaceous Separation Point Suite, New Zealand, using U/Pb isotopes, REE and Ti geothermometry. Contrib Mineral Petrol 156(2):133–160

Brewer RA, Vervoort JD, Lewis RS, Gaschnig RM, Hart GL (2008) New constraints on the extent of Paleoproterozoic and Archean basement in the northwest U.S. Cordilllera. EOS, Transactions, American Geophysical Union, Fall Meeting Supplement 89(53), Abstract T23C-2066

Burchfiel BC, Cowan DS, Davis GA (1992) Tectonic overview of the Cordilleran orogen in the western United States. In: Burchfiel BC, Lipman PW, Zoback ML (eds) The Cordilleran orogen: conterminous U.S. Geol N Am G-3:407–479

Carr SD (1992) Tectonic setting and U-Pb geochronology of the early Tertiary Ladybird Leucogranite Suite, Thor-Odin—Pinnacles area, southern Omineca Belt, British Columbia. Tectonics 11(2):258–278

Chang Z, Vervoort JD, McClelland WC, Knaack C (2006) U-Pb dating of zircon by LA-ICP-MS. Geochem Geophys Geosyst 7(1):Q05009

Chase RB, Bickford ME, Tripp SE (1978) Rb-Sr and U-Pb isotopic studies of the northeastern Idaho Batholith and border zone. Geol Soc Am Bull 89(9):1325–1334

Cheney JT, Webb AAG, Coath CD, McKeegan KD (2004) In situ ion microprobe $^{207}Pb/^{206}Pb$ dating of monazite from Precambrian metamorphic suites, Tobacco Root Mountains, Montana. In: Brady JB, Burger HR, Cheney JT, Harms TA (eds) Precambrian geology of the tobacco root mountains, Montana. Geol Soc Am Spec Pap 377:151–179

Coleman DS, Glazner AF (1997) The Sierra Crest magmatic event; rapid formation of juvenile crust during the Late Cretaceous in California. Int Geol Rev 39(9):768–787

Coleman DS, Gray W, Glazner AF (2004) Rethinking the emplacement and evolution of zoned plutons: geochronologic evidence for incremental assembly of the Tuolumne Intrusive Suite, California. Geology 32(5):433–436

Crawford ML, Crawford WA, Lindline J (2005) 105 Million years of igneous activity, Wrangell, Alaska, to Prince Rupert, British Columbia. Can J Earth Sci 42:1097–1116

Criss RE, Fleck RJ (1987) Petrogenesis, geochronology, and hydrothermal systems of the northern Idaho batholith and adjacent areas based on $^{18}O/^{16}O$, D/H, $^{87}Sr/^{86}Sr$, K-Ar, and $^{40}Ar/^{39}Ar$ studies. In: Vallier TL, Brooks HC (eds) Geology of the Blue Mountains region of Oregon, Idaho, and Washington; the Idaho Batholith and its border zone. U.S. Geological Survey Professional Paper 1436, pp 95–137

Criss RE, Lanphere MA, Taylor HP Jr (1982) Effects of regional uplift, deformation, and meteoric-hydrothermal metamorphism on K-Ar ages of biotites in the southern half of the Idaho Batholith. J Geophys Res 87(8):7029–7046

DeCelles PG (2004) Late Jurassic to Eocene evolution of the Cordilleran thrust belt and foreland basin system, western U.S.A. Am J Sci 304(2):105–168

DeCelles PG, Ducea MN, Kapp P, Zandt G (2009) Cyclicity in Cordilleran orogenic systems. Nat Geosci 2:251–257

DeGraaff-Surpless K, Graham SA, Wooden JL, McWilliams MO (2002) Detrital zircon provenance analysis of the Great Valley Group, California: evolution of an arc-forearc system. Geol Soc Am Bull 114(12):1564–1580

Dickinson WR, Gehrels GE (2003) U-Pb ages of detrital zircons from Permian and Jurassic eolian sandstones of the Colorado Plateau, USA: paleogeographic implications. Sediment Geol 163(1–2):29–66

Dickinson WR, Klute MA, Hayes MJ, Janecke SU, Lundin ER, McKittrick MA, Olivares MD (1988) Paleogeographic and paleotectonic setting of Laramide sedimentary basins in the central Rocky Mountain region. Geol Soc Am Bull 100(7):1023–1039

Doughty PT, Chamberlain KR (1996) Salmon River Arch revisited: new evidence for 1370 Ma rifting near the end of deposition in the Middle Proterozoic Belt Basin. Can J Earth Sci 33:1037–1052

Duke GI (2009) Black Hills-Alberta carbonatite-kimberlite linear trend: slab edge at depth? Tectonophysics 464(1–4):186–194

Eggins SM, Kinsley LPJ, Shelley JMG (1998) Deposition and element fractionation processes during atmospheric pressure laser sampling for analysis by ICP-MS. Appl Surf Sci 127–129:278–286

Evans KV, Zartman RE (1990) U-Th-Pb and Rb-Sr geochronology of middle Proterozoic granite and augen gneiss, Salmon River Mountains, east-central Idaho. Geol Soc Am Bull 102(1):63–73

Feeley TC (2003) Origin and tectonic implications of across-strike geochemical variations in the Eocene Absaroka Volcanic Province, United States. J Geol 111(3):329–346

Fisher FS, McIntyre DH, Johnson KM (1992) Geologic Map of the Challis 1° × 2° quadrangle, Idaho. U.S. Geological Survey Miscellaneous Investigation Series Map I-1819

Fleck RJ, Criss RE (2004) Location, age, and tectonic significance of the Western Idaho suture zone (WISZ). U.S. Geological Survey Open-File Report 2004-1039, 48 p

Foster DA, Fanning CM (1997) Geochronology of the northern Idaho batholith and the Bitterroot metamorphic core complex; magmatism preceding and contemporaneous with extension. Geol Soc Am Bull 109(4):379–394

Foster DA, Hyndman DW (1990) Magma mixing and mingling between synplutonic mafic dikes and granite in the Idaho-Bitterroot Batholith. In: Anderson JL (ed) The nature and origin of Cordilleran magmatism. Geol Soc Am Mem 174:347–358

Foster DA, Schafer C, Fanning CM, Hyndman DW (2001) Relationships between crustal partial melting, plutonism, orogeny, and exhumation; Idaho-Bitterroot batholith. Tectonophysics 342(3–4):313–350

Foster DA, Mueller PA, Mogk DW, Wooden JL, Vogl JJ (2006) Proterozoic evolution of the western margin of the Wyoming craton: implications for the tectonic and magmatic evolution of the northern Rocky Mountains. Can J Earth Sci 43:1601–1619

Foster DA, Doughty PT, Kalakay TJ, Fanning CM, Coyner S, Grice WC, Vogl J (2007a) Kinematics and timing of exhumation of metamorphic core complexes along the Lewis and Clark fault zone, northern Rocky Mountains, USA. In: Till AB, Roeske SM, Sample JC, Foster DA (eds) Exhumation associated with continental strike-slip fault systems. Geol Soc Am Spec Pap 434:207–232

Foster DA, Kalakay TJ, Mueller PA, Heatherington AL (2007b) Late Cretaceous granitic plutons in southwestern Montana. Northwest Geol 36:73–90

Friedman RM, Armstrong RL (1995) Jurassic and Cretaceous geochronology of the southern Coast Belt, British Columbia, 49 degrees to 51 degrees N. In: Miller DM, Busby CJ (eds) Jurassic magmatism and tectonics of the North American Cordillera. Geol Soc Am Spec Pap 299:95–139

Gaschnig RM, Vervoort JD, Lewis RS, Dufrane SA (2008) Utilizing U-Pb geochronology of inherited zircon in the Atlanta lobe of the Idaho batholith as a probe of the deep crust in southern Idaho: a progress report. Northwest Geol 37:101–110

Gehrels G, Rusmore M, Woodsworth G, Crawford M, Andronicos C, Hollister L, Patchett J, Ducea M, Butler R, Klepeis K, Davidson C, Friedman R, Haggart J, Mahoney B, Crawford W, Pearson D, Girardi J (2009) U-Th-Pb geochronology of the Coast Mountains batholith in north-coastal British Columbia: constraints on age and tectonic evolution. Geol Soc Am Bull 121(9–10):1341–1361

Getty SR, Selverstone J, Wernicke BP, Jacobsen SB, Aliberti E, Lux DR (1993) Sm–Nd dating of multiple garnet growth events in an arc-continent collision zone, northwestern U.S. Cordillera. Contrib Mineral Petrol 115(1):45–57

Giorgis S, Tikoff B, McClelland W (2005) Missing Idaho arc; transpressional modification of the $^{87}Sr/^{86}Sr$ transition on the western edge of the Idaho Batholith. Geology 33(6):469–472

Giorgis S, McClelland W, Fayon A, Singer BS, Tikoff B (2008) Timing of deformation and exhumation in the western Idaho shear zone, McCall, Idaho. Geol Soc Am Bull 120(9):1119–1133

Glazner AF (2007) Thermal limitations on incorporation of wall rock into magma. Geology 35(4):319–322

Gordon SM, Whitney DL, Teyssier C, Gove M, Dunlap WJ (2008) Timescales of migmatization, melt crystallization, and cooling in a Cordilleran gneiss dome: Valhalla complex, southeastern British Columbia. Tectonics 27:TC4010

Hinchey AM, Carr SD, McNeill PD, Rayner N (2006) Paleocene-Eocene high-grade metamorphism, anatexis, and deformation in the Thor-Odin dome, Monashee complex, southeastern British Columbia. Can J Earth Sci 43:1341–1365

Hoskin PWO, Schaltegger U (2003) The composition of zircon and igneous and metamorphic petrogenesis. In: Hanchar JM, Hoskin PWO (eds) Zircon. Rev Mineral Geochem 53:27–62

House MA, Hodges KV, Bowring SA (1997) Petrological and geochronological constraints on regional metamorphism along the northern border of the Bitterroot batholith. J Metamorph Geol 15:753–764

House MA, Bowring SA, Hodges KV (2002) Implications of middle Eocene epizonal plutonism for the unroofing history of the Bitterroot metamorphic core complex, Idaho-Montana. Geol Soc Am Bull 114(4):448–461

Hyndman DW (1983) The Idaho batholith and associated plutons, Idaho and western Montana. In: Roddick JA (ed) Circum-Pacific plutonic terranes. Geol Soc Am Mem 159:213–240

Hyndman DW (1984) A petrographic and chemical section through the northern Idaho Batholith. J Geol 92(1):83–102

Hyndman DW, Foster DA (1988) The role of tonalites and mafic dikes in the generation of the Idaho batholith. J Geol 96(1):31–46

Janecke SU (1992) Kinematics and timing of three superposed extensional systems, east central Idaho; evidence for an Eocene tectonic transition. Tectonics 11:1121–1138

Janecke SU, Snee LW (1993) Timing and episodicity of middle Eocene volcanism and onset of conglomerate deposition, Idaho. J Geol 101:603–621

Janecke SU, Hammond BF, Snee LW, Geissman JW (1997) Rapid extension in an Eocene volcanic arc; structure and paleogeography of an intra-arc half graben in central Idaho. Geol Soc Am Bull 109(3):253–267

Jordan BT (1994) Emplacement and exhumation of the southeastern Atlanta lobe of the Idaho batholith and outlying stocks, south-central Idaho. MS thesis, Idaho State University, 110 p

Kauffman JD, Garwood DL, Schmidt KL, Lewis RS, Othberg KL, Phillips WM (2006) Geologic map of the Idaho parts of the Orofino and Clarkston 30 × 60 minute quadrangles. Idaho Geological Survey Digital Web Map 69

Kiilsgaard TH, Lewis RS (1985) Plutonic rocks of Cretaceous age and faults in the Atlanta Lobe of the Idaho batholith, Challis quadrangle. In: McIntyre DH (ed) Symposium on the geology and mineral deposits of the Challis 1°× 2° quadrangle, Idaho. U.S. Geological Survey Bulletin 1658, pp 29–42

Kiilsgaard TH, Lewis RS, Bennett EH (2001) Plutonic and hypabyssal rocks of the Hailey 1° × 2° quadrangle, Idaho. U.S. Geological Survey Bulletin 2064-U, 18 p

King EM, Valley JW (2001) The source, magmatic contamination, and alteration of the Idaho Batholith. Contrib Mineral Petrol 142(1):72–88

King EM, Beard BL, Valley JW (2007) Strontium and oxygen isotopic evidence for strike/slip movement of accreted terranes in the Idaho batholith. Lithos 96(3–4):387–401

Kosler J, Sylvester PJ (2003) Present trends and the future of zircon in geochronology: laser ablation ICPMS. In: Hanchar JM, Hoskin PWO (eds) Zircon. Rev Mineral Geochem 53:243–276

Kruckenberg SC, Whitney DL, Teyssier C, Fanning CM, Dunlap WJ (2008) Paleocene-Eocene migmatite crystallization, extension, and exhumation in the hinterland of the northern Cordillera: Okanogan dome, Washington, USA. Geol Soc Am Bull 120(7):912–929

Larson PB, Geist DJ (1995) On the origin of low-^{18}O magmas: evidence from the Casto pluton, Idaho. Geology 23(10):909–912

Lee RG (2004) The geochemistry, stable isotopic composition, and U-Pb geochronology of tonalite trondhjemites within the accreted terrane, near Greer, north-central Idaho. MS thesis, Washington State University, 132 p

Leeman WP, Menzies MA, Matty DJ, Embree GF (1985) Strontium, neodymium and lead isotopic compositions of deep crustal xenoliths from the Snake River Plain: evidence for Archean basement. Earth Planet Sci Lett 75(4):354–368

Lewis RS, Kiilsgaard TH (1991) Eocene plutonic rocks in south central Idaho. J Geophys Res 96(B8):13295–13311

Lewis RS, Stanford LR (2002) Geologic map compilation of the Hamilton 30 × 60 minute quadrangle, Idaho. Idaho Geological Survey Geologic Map 32

Lewis RS, Kiilsgaard TH, Bennett EH, Hall WE (1987) Lithologic and chemical characteristics of the central and southeastern part of the southern lobe of the Idaho Batholith. In: Vallier TL, Brooks HC (eds) Geology of the Blue Mountains region of Oregon, Idaho, and Washington; the Idaho batholith and its border zone. U.S. Geological Survey Professional Paper 1436, pp 171–196

Lewis RS, Burmester RF, Kauffman JD, Breckenridge RM, Schmidt KL, McFaddan MD, Myers PE (2007a) Geologic map of the Kooskia 30 × 60 minute quadrangle, Idaho. Idaho Geological Survey Digital Web Map 93

Lewis RS, Burmester RF, McFaddan MD, Kauffman JD, Doughty PT, Oakley WL, Frost TP (2007b) Geologic map of the Headquarters 30 × 60 minute quadrangle, Idaho. Idaho Geological Survey Digital Web Map 92

Link PK, Durk KM, Fanning CM (2007) SHRIMP U-Pb ages for Archean orthogneiss, Mesoproterozoic paragneiss, and Eocene Boulder Creek pluton, Pioneer Mountains, south-central Idaho, part of the 2600 Grouse Creek block. Abstr Programs Geol Soc Am 39(6):613

Ludwig KR (2001) Squid version 1.02: a users manual. Berkeley Geochronol Cent Spec Publ 1:1–22

Ludwig KR (2003) User's manual for Isoplot 3.00: a geochronological toolkit for Microsoft Excel. Berkeley Geochronol Cent Spec Publ 4:1–70

Lund K, Snee LW (1988) Metamorphism, structural development, and age of the continental-island arc juncture in west-central Idaho. In: Ernst WG (ed) Metamorphism and crustal evolution, western conterminous United States. Rubey Volume 7:296–331

Lund K, Aleinikoff JN, Kunk MJ, Unruh DM, Zeihen GD, Hodges WC, Du Bray EA, O'Neill MO (2002) SHRIMP U-Pb and ^{40}Ar/^{39}Ar age constraints for relating plutonism and mineralization in the Boulder Batholith region, Montana. Econ Geol 97(2):241–267

Lund K, Aleinikoff JN, Evans KV, Fanning CM (2003) SHRIMP U-Pb geochronology of Neoproterozoic Windermere Supergroup, central Idaho: Implications for rifting of western Laurentia and synchroneity of Sturtian glacial deposits. Geol Soc Am Bull 115(3):349–372

Lund K, Aleinikoff JN, Yacob EY, Unruh DM, Fanning CM (2008) Coolwater culmination: sensitive high-resolution ion microprobe (SHRIMP) U-Pb and isotopic evidence for continental delamination in the Syringa Embayment, Salmon River suture, Idaho. Tectonics 27(TC2009)

Manduca CA, Silver LT, Taylor HP Jr (1992) ^{87}Sr/^{86}Sr and ^{18}O/^{16}O isotopic systematics and geochemistry of granitoid plutons across a steeply-dipping boundary between contrasting lithospheric blocks in western Idaho. Contrib Mineral Petrol 109(3):355–372

Manduca CA, Kuntz MA, Silver LT (1993) Emplacement and deformation history of the western margin of the Idaho batholith near McCall, Idaho; influence of a major terrane boundary. Geol Soc Am Bull 105(6):749–765

McClelland WC, Oldow JS (2007) Late Cretaceous truncation of the western Idaho shear zone in the central North American Cordillera. Geology 35(8):723–726

McClelland WC, Tikoff B, Manduca CA (2000) Two-phase evolution of accretionary margins: examples from the North American Cordillera. Tectonophysics 326(1–2):37–55

McKervey A (1998) The petrogenesis of the Eocene Challis Volcanic Group, Idaho, western U.S.A. PhD dissertation, The Open University (UK), 371 p

Miller FK, Burmester RF, Powell RE, Miller DM, Derkey PD (1999) Digital geologic map of the Sandpoint1- by 2-degree quadrangle, Washington, Idaho, and Montana. US Geological Survey Open-File Report 99-144

Miller JS, Matzel JEP, Miller CF, Burgess SD, Miller RB (2007) Zircon growth and recycling during the assembly of large, composite arc plutons. J Volcanol Geotherm Res 167(1–4):282–299

Mitchell TA (1997) Petrology, geochemistry, and petrogenesis of the Eocene Big Smoky Creek Stock, south-central Idaho. M.S. thesis, Washington State University

Mueller PA, Heatherington AL, D'Arcy KA, Wooden JL, Nutman AP (1996) Contrasts between Sm-Nd whole-rock and U-Pb zircon systematics in the Tobacco Root batholith, Montana: implications for the determination of crustal age provinces. Tectonophysics 265:169–179

Murphy JG, Foster DA, Kalakay TJ, John BE, Hamilton M (2002) U-Pb zircon geochronology of the eastern Pioneer igneous complex, SW Montana: magmatism in the foreland of the Cordilleran fold and thrust belt. Northwest Geol 31:1–12

Ortega-Rivera A (2003) Geochronological constraints on the tectonic history of the Peninsular Ranges batholith of Alta and Baja California; tectonic implications for western Mexico. In: Johnson SE, Paterson SR, Fletcher JM, Girty GH, Kimbrough DL, Martin-Barajas A (eds) Tectonic evolution of northwestern Mexico and the southwestern USA. Geol Soc Am Spec Pap 374:297–335

Ortega-Rivera A, Farrar E, Hanes JA, Archibald DA, Gastil RG, Kimbrough DL, Zentilli M, Lopez-Martinez M, Feraud G, Ruffet G (1997) Chronological constraints on the thermal and tilting history of the Sierra San Pedro Martir pluton, Baja California, Mexico, from U/Pb, 40Ar/39Ar, and fission-track geochronology. Geol Soc Am Bull 109(6):728–745

Paces JB, Miller JD (1993) Precise U-Pb ages of Duluth Complex and related mafic intrusions, north-eastern Minnesota: geochronological insights to physical, petrogenetic, paleomagnetic, and tectonomagmatic processes associated with the 1.1 Ga midcontinental rift system. J Geophys Res 98:13997–14013

Reid MR, Coath CD, Mark Harrison T, McKeegan KD (1997) Prolonged residence times for the youngest rhyolites associated with Long Valley Caldera: ^{230}Th–^{238}U ion microprobe dating of young zircons. Earth Planet Sci Lett 150(1–2):27–39

Reppe TH (1997) Geology, geochemistry, and petrogenesis of the Eocene Prairie Creek Stock, Smoky Mountains, Blaine and Camas Counties, Idaho. M.S. thesis, Washington State University

Robertson MC (1997) Geochemistry and petrogenesis of the Eocene Boulder Mountain Stock, central Idaho. M.S. thesis, Washington State University

Saleeby J (2003) Segmentation of the Laramide Slab: evidence from the southern Sierra Nevada region. Geol Soc Am Bull 115(6):655–668

Saleeby JB, Ducea MN, Busby CJ, Nadin ES, Wetmore PH (2008) Chronology of pluton emplacement and regional deformation in the southern Sierra Nevada batholith, California. In: Wright JE, Shervais JW (eds) Ophiolites, arcs, and batholiths: a tribute to Cliff Hopson. Geol Soc Am Spec Pap 438:397–427

Schmidt KL (1994) Geology and petrology of the Eocene Ibex Canyon igneous complex, Custer and Blaine counties, Idaho. MS thesis, Idaho State University, 177 p

Selverstone J, Wernicke BP, Aliberti EA (1992) Intracontinental subduction and hinged unroofing along the Salmon River Suture Zone, central Idaho. Tectonics 11(1):124–144

Sevigny JH, Parrish RR, Ghent ED (1989) Petrogenesis of peraluminous granites, Monashee Mountains, southeastern Canadian Cordillera. J Petrol 30(3):557–581

Shuster RD, Bickford ME (1985) Chemical and isotopic evidence for the petrogenesis of the northeastern Idaho batholith. J Geol 93(6):727–742

Simon JI, Reid MR (2005) The pace of rhyolite differentiation and storage in an 'archetypical' silicic magma system, Long Valley, California. Earth Planet Sci Lett 235:123–140

Simon JI, Renne PR, Mundil R (2008) Implications of pre-eruptive magmatic histories of zircons for U-Pb geochronology of silicic extrusions. Earth Planet Sci Lett 266(1–2):182–194

Simonsen SW (1997) 40Ar/39Ar ages of Eocene dikes and the age of extension in a Tertiary magmatic arc, Idaho and Montana. MS thesis, University of Montana

Sims PK, Lund K, Anderson E (2005) Precambrian crystalline basement map of Idaho—an interpretation of aeromagnetic anomalies. U.S. Geological Survey Scientific Investigation Map 2884

Snee LW, Kunk MJ (1989) ^{40}Ar/^{39}Ar thermochronology of mineral deposits in the southern part of the Idaho batholith. U.S. Geological Survey Open-File Report 89-639, pp 37–38

Snee LW, Lund K, Sutter JF, Balcer DE, Evans KV (1995) An ^{40}Ar/^{39}Ar chronicle of the tectonic development of the Salmon River suture zone, western Idaho. In: Vallier TL, Brooks HC (eds) Geology of the Blue Mountains Region of Oregon, Idaho, and Washington: petrology and tectonic evolution of pre-tertiary rocks of the Blue Mountains Region, U.S. Geological Survey Professional Paper 1438, pp 359–414

Snee LW, Davidson GF, Unruh DM (2007) Geological, geochemical, and ^{40}Ar/^{39}Ar and U-Pb thermochronological constraints for the tectonic development of the Salmon River suture zone near Orofino, Idaho. In: Kuntz MA, Snee LW (eds) Geological studies of the Salmon River suture zone and adjoining areas, west-central Idaho and eastern Oregon. U.S. Geological Survey Professional Paper 1738, pp 51–94

Taubeneck WH (1971) Idaho batholith and its southern extension. Geol Soc Am Bull 82(7):1899–1928

Toth MI, Stacey JS (1992) Constraints on the formation of the Bitterroot lobe of the Idaho batholith, Idaho and Montana, from U-Pb zircon geochronology and feldspar Pb isotopic data. U.S. Geological Survey Bulletin 2008, 14 p

Tulloch AJ, Kimbrough DL (2003) Paired plutonic belts in convergent margins and the development of high Sr/Y magmatism: Peninsular Ranges batholith of Baja-California and Median batholith of New Zealand. In: Johnson SE, Paterson SR, Fletcher JM, Girty GH, Kimbrough DL, Martin-Barajas A (eds) Tectonic evolution of northwestern Mexico and the southwestern USA. Geol Soc Am Spec Pap 374:275–295

Unruh DM, Lund K, Snee LW, Kuntz MA (2008) Uranium-lead zircon ages and Sr, Nd, and Pb isotope geochemistry of selected plutonic rocks from western Idaho. US Geological Survey Open-file Report 2008-1142, 42 p

Vanderhaeghe O, Teyssier C, Wysoczanski R (1999) Structural and geochronological constraints on the role of partial melting during the formation of the Shuswap metamorphic core complex at the latitude of the Thor-Odin Dome, British Columbia. Can J Earth Sci 36:917–943

Vazquez J, Reid M (2002) Time scales of magma storage and differentiation of voluminous high-silica rhyolites at Yellowstone caldera, Wyoming. Contrib Mineral Petrol 144(3):274–285

Walker BA Jr, Miller CF, Lowery Claiborne L, Wooden JL, Miller JS (2007) Geology and geochronology of the Spirit Mountain batholith, southern Nevada: Implications for timescales and physical processes of batholith construction. J Volcanol Geotherm Res 167(1–4):239–262

Whitehouse MJ, Stacey JS, Miller FK (1992) Age and nature of the basement in northeastern Washington and northern Idaho: isotopic evidence from Mesozoic and Cenozoic granitoids. J Geol 100:691–701

Williams LD (1977) Petrology and petrography of a section across the Bitterroot lobe of the Idaho batholith. Ph.D. thesis, University of Montana, Missoula, 221 p

Williams IS (1998) U-Th-Pb geochronology by ion microprobe. Reviews in Economic Geology 7:1–35

Wolf DE, Leeman WP, Vervoort JD (2005) U-Pb zircon geochronology of crustal xenoliths confirms presence of Archean basement beneath the central and eastern Snake River Plain. Geol Soc Am Abstr Programs 37(7):60